

Table 1
Candidate transcription factors that regulate molecular pathways activated in HCC.

SAGE library	Transcription factor	Molecular processes	P-value
HCC-HCV	NF- κ B	Antigen presentation	0.004
		Antigen processing	
		Defense response	
		Immune response	
	SREBF1	Cholesterol biosynthesis	0.05
		Lipid biosynthesis	
		β -Glucoside transport	
	SP1	Negative regulation of lipoprotein metabolism	0.05
		Electron transport; drug metabolism	
		Oxygen and reactive oxygen species metabolism	
IRF1	Cell-substrate junction assembly; wound healing	0.05	
	Immune response		
	Antigen presentation; antigen processing		
HCC-HBV	HNF4- α	Defense response; positive regulation of cell	0.002
		Lipid transport	
	HNF1	Fatty acid metabolism	0.01
		Smooth muscle cell proliferation	
		Acute-phase response; lipid transport	
	SP1	Negative regulation of lipid catabolism	0.01
		β -Glucoside transport	
		Negative regulation of lipoprotein metabolism	
	c-Jun	Zinc ion homeostasis; response to biotic stimulus	0.03
		Nitric oxide mediated signal transduction	
		Copper ion homeostasis; fatty acid biosynthesis	
	C/EBP- α	Progesterone catabolism; progesterone metabolism	0.03
		Regulation of lipid metabolism;	
		Prostaglandin metabolism	
	SREBF1	Lipid transport; negative regulation of lipid catabolism	0.03
		Negative regulation of lipoprotein metabolism	
		β -Glucoside transport	
c-Myc	Positive regulation of interleukin-8 biosynthesis	0.03	
	Lipid biosynthesis; fatty acid biosynthesis		
	Fatty acid metabolism		
USF1	Negative regulation of lipid catabolism	0.03	
	Negative regulation of lipoprotein metabolism		
	Fatty acid biosynthesis; fatty acid metabolism		
PPAR- α	Fatty acid desaturation;	0.03	
	Activation of pro-apoptotic gene products		
	Release of cytochrome c from mitochondria		
COUP-TFI	Fatty acid metabolism	0.03	
	Smooth muscle cell proliferation		
	Fatty acid metabolism		
C/EBP- β	Smooth muscle cell proliferation	0.03	
	Lipid transport		
	Smooth muscle cell proliferation		
	Acute-phase response	0.03	
	Regulation of interleukin-6 biosynthesis		
	Fat cell differentiation		
		Inflammatory response	

These findings were evaluated by other pathway analysis software, Ingenuity Pathways Analysis (IPA). We applied the signaling network analysis to the transcripts up-regulated in the HCC libraries ($P < 0.005$). We found that the top signaling network activated in HCC-HBV contained several pathways involved in ERK/MAPK signaling, PPAR signaling, linoleic acid metabolism, and fatty acid metabolism (Supplemental Fig. 2A). Similarly, pathways involved in interferon signaling, NF- κ B signaling, antigen presentation, PPAR signaling, linoleic

acid metabolism, and fatty acid metabolism were included in the top signaling network activated in HCC-HCV (Supplemental Fig. 2B). Consistent with the results of transcription factor analysis by MetaCoreTM, pathway analysis indicated that SREBF1 participates in the lipogenesis pathway in both HCC-HBV and HCC-HCV (blue nodes in Supplemental Fig. 2A and B). SREBF1, a major regulator of the lipogenesis pathway, binds to sterol regulatory elements on the genome [30], but less is known about its role in

HCC [31]. We therefore focused on the role of *SREBF1* signaling in HCC.

3.3. Validation of SAGE and signaling network analysis

We performed real-time RT-PCR analysis of *SREBF1* and three representative target genes (*SCD*, *FADS1*, and *FASN*) [20] on 44 samples not used for SAGE. We found that the levels of *SREBF1*, *SCD*, and *FASN* mRNAs were higher in HCC tissues and CLD tissues compared with normal liver, and that these differences were statistically significant (Fig. 1A). We further compared the expression of *SREBF1*, *FADS1*, and *FASN* between HCC and non-cancerous liver tissues, and identified the overexpression of *SREBF1* in HCC with statistical significance (Supplemental Fig. 3). Scatter plot analysis showed that the expression levels of *SREBF1* were correlated with those of *FADS1* ($R = 0.57$, $P < 0.0001$), *SCD* ($R = 0.82$, $P < 0.0001$), and *FASN* ($R = 0.74$, $P < 0.0001$) (Fig. 1B).

Since the mammalian genome encodes two *SREBF1* isoforms, *SREBF1a* and *SREBF1c* [22], we performed semi-quantitative RT-PCR with isoform specific primers to determine which of these isoforms was up-regulated in HCC. We found that *SREBF1c* mRNA, but not *SREBF1a* mRNA, was up-regulated in HCC compared with adjacent non-cancerous liver and normal liver tissues (Supplemental Fig. 4A).

3.4. Functional assay of the lipogenesis pathway in cell lines

Although genome-wide expression profiling showed that the lipogenesis pathway was activated in HCC possibly through up-regulation of *SREBF1*, it was not clear that this pathway played a role in HCC growth. To investigate the role of lipogenesis in HCC cell proliferation, we transfected two short interfering (si)-RNAs (*SREBF1-1* and *SREBF1-2*) targeting *SREBF1* into the HuH7 and Hep3B cells. These cell lines have no chromosome amplification or deletion on 17p11, on which *SREBF1* is located [32]. Transfection of the si-RNA constructs for *SREBF1-1* or *SREBF1-2* decreased expression of *SREBF1* 90% and 70%, respectively, and the expression of both *SCD* and *FADS1* 70% and 60%, respectively (Fig. 2A). Because differences in *SREBF1c* and *SREBF1a* sequence alignments are very small, we could not design si-RNAs specifically targeting *SREBF1c*. We therefore checked the effect of si-RNAs on the expression of the *SREBF1* isoforms. We found that the expression of *SREBF1c* was relatively more suppressed than that of *SREBF1a* (Supplemental Fig. 4B), which may have been associated with the higher expression of *SREBF1a* than *SREBF1c* in cultured cell lines [25].

We found that the growth of these transfected cells was significantly inhibited at 72 h compared with mock transfected cells (Fig. 2B and Supplemental Fig. 5A). Examination of anchorage independent cell growth showed strong suppression by deactivation of the lipogenesis pathway (Fig. 2C). Because insulin-like growth factor (IGF) is known to induce cancer cell proliferation through activation of PI3-kinase signaling followed by *SREBF1* induction, we investigated the effect of *SREBF1* knockdown on IGF2 mediated cell proliferation. Interestingly, *SREBF1* knockdown abrogated the IGF2 dependent cell proliferation (Supplemental Fig. 5B). Moreover, both the TUNEL assay and annexin V staining showed that transfection of *SREBF1* si-RNAs increased apoptosis compared with mock transfected cells (Fig. 2D and E).

We further investigated the role of *SREBF1* overexpression on cell growth *in vitro*. We transiently transfected control pCMV7 plasmids or pCMV7-*SREBF1c* plasmids (Fig. 3A), and cell proliferation was enhanced in *SREBF1* overexpressing cells compared with the control in both HuH7 and Hep3B cells evaluated by focus assay (Fig. 3B and supplemental Fig. 6). Furthermore, overexpression of *SREBF1* intensified the phosphorylation of GSK-3 β , one of the major kinase phosphorylated by the activation of IGF signaling, in a dose-dependent manner (Fig. 3C).

3.5. *SREBF1* Expression and prognosis

Since the above results indicated that *SREBF1* signaling may play an important role on tumor cell growth, we investigated the relationship between *SREBF1* expression and mortality in 54 HCC patients by IHC. When we examined the expression of *SREBF1* in HCC tissues and adjacent non-cancerous liver tissues, we identified the increase of the cytoplasmic *SREBF1* staining in a subset of HCC (Fig. 4A). We evaluated the expression of *SREBF1* in HCC and classified 4, 30, and 20 HCCs as *SREBF1*-negative, *SREBF1*-low, and *SREBF1*-high HCC, respectively (Fig. 4B and Supplemental Fig. 1). We could not detect any differences of clinico-pathological characteristics between *SREBF1*-high HCC and *SREBF1*-low/-negative HCC including histological steatosis (Supplemental Table 4). Since the seven of these HCC samples were also used for real-time RT-PCR analysis, we investigated the relation of *SREBF1* RNA and protein expression (Fig. 4C). *SREBF1* RNA expression was significantly higher in *SREBF1*-high HCC than in *SREBF1*-low/-negative HCC with statistical significance ($P = 0.03$). Then we examined the cell proliferation of these HCC samples by PCNA staining. Notably, PCNA indexes were significantly higher in *SREBF1*-high HCC than *SREBF1*-low/-negative HCC with statistical significance ($P < 0.001$) (Fig. 4D). We further investigated the relationship between *SREBF1*

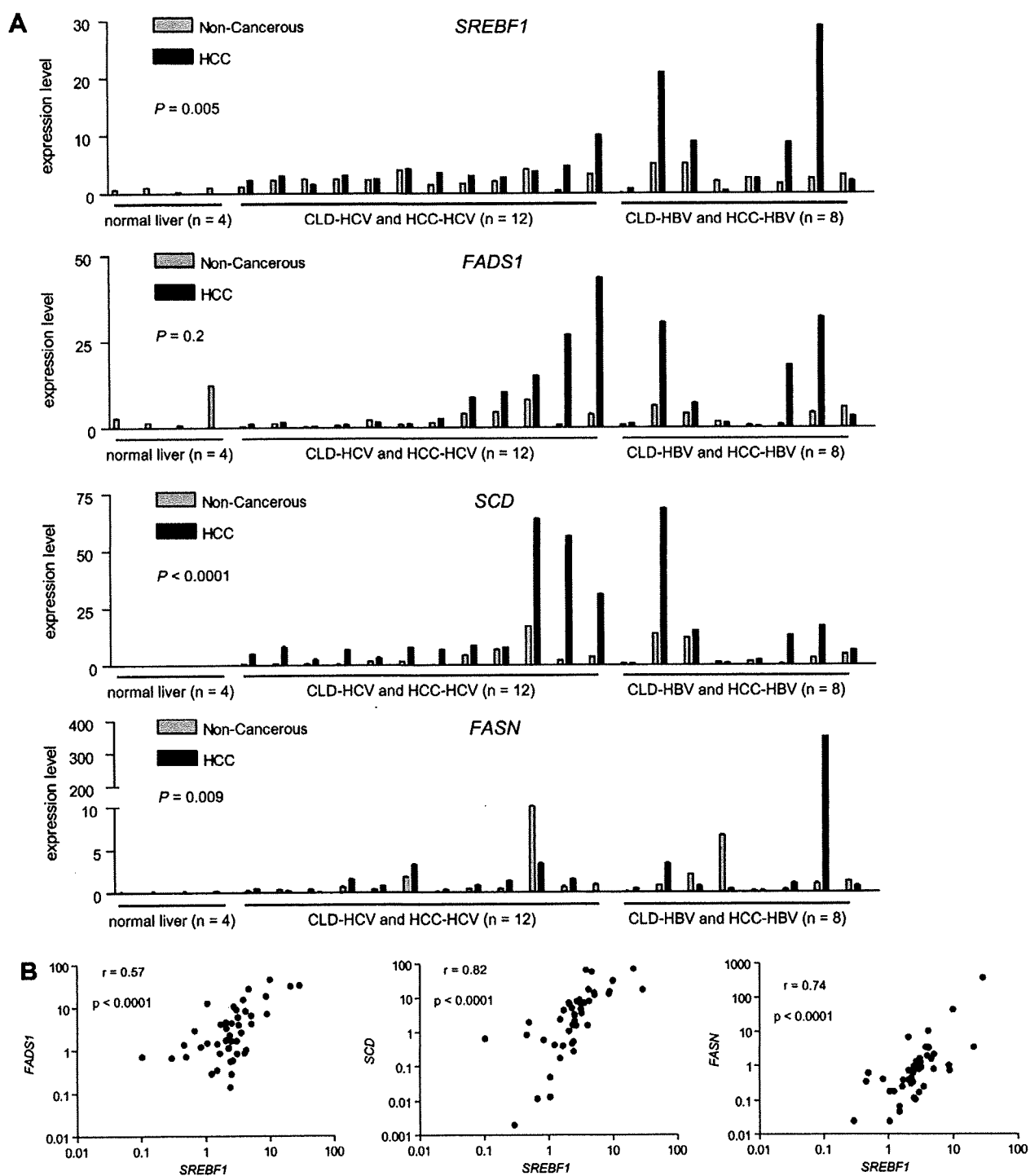


Fig. 1. (A) Real-time quantitative RT-PCR analysis. RNA was isolated from 44 tissue samples: 20 HCC, 20 corresponding CLD, and four normal liver samples. Differential expression of each gene among normal liver tissues, CLD tissues, and HCC tissues was examined by Kruskal–Wallis tests. (B) Scatter plot analysis. Gene expression levels of *FADS1*, *SCD* and *FASN* were well-correlated with those of *SREBF1*, as shown by Spearman’s correlation coefficients.

protein expression and prognosis. Kaplan–Meier survival analysis showed a significant relationship between poor survival and high *SREBF1* protein expression

($P = 0.04$; Fig. 4E). Univariate Cox regression analysis showed a correlation between high *SREBF1* protein expression and high risk of mortality with statistical

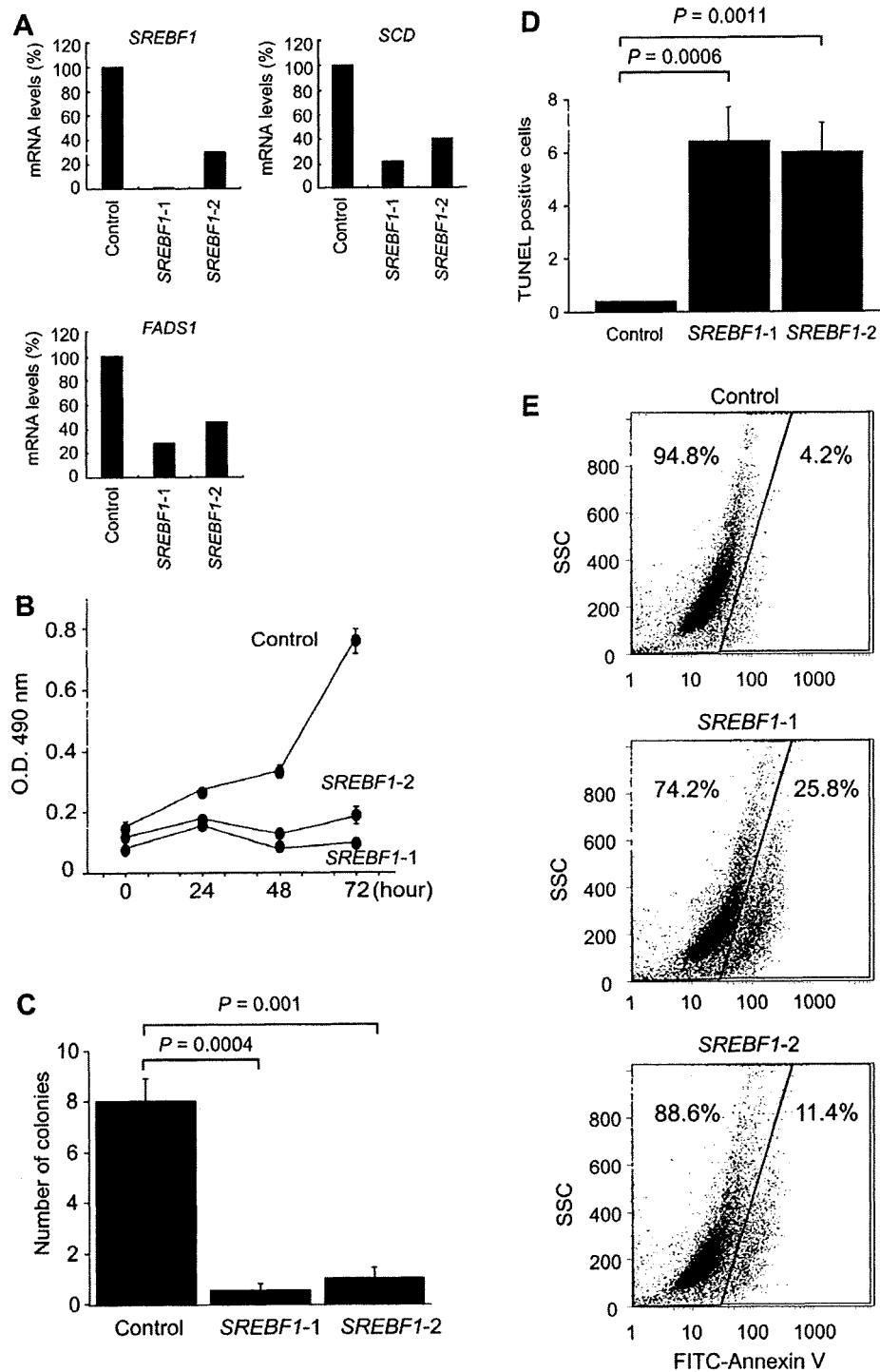


Fig. 2. (A) Effect of RNA interference targeting *SREBF1* in HuH7 cells. Expression levels of *SREBF1* mRNA were reduced by si-RNAs targeting different exons in *SREBF1*. Transcripts of *FADS1* and *SCD* were also down-regulated, showing transcriptional deactivation of the lipogenesis pathway. (B) Cell proliferation assay. Deactivation of the lipogenesis pathway severely reduced cell growth in HuH7 cells. (C) Soft agar assay. Deactivation of the lipogenesis pathway inhibited anchorage independent cell growth in HuH7 cells. (D) TUNEL assay. Deactivation of the lipogenesis pathway significantly increased the number of TUNEL-positive cells in HuH7 cells. (E) Annexin V staining evaluated by flow cytometer. Deactivation of the lipogenesis pathway significantly increased the number of annexin V positive cells in HuH7 cells.

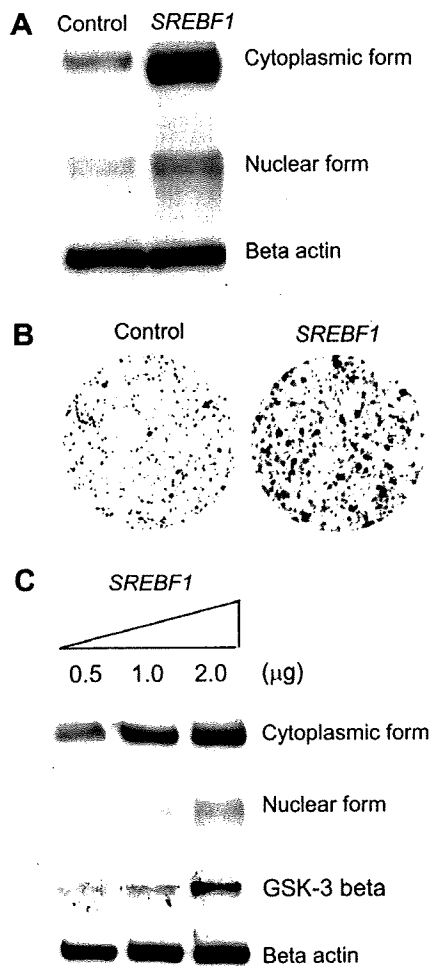


Fig. 3. (A) Western blot analysis of *SREBF1* protein expression in HuH7 cells transfected with control pCMV7 plasmids or pCMV7-*SREBF1c* plasmids. Both cytoplasmic and nuclear forms of *SREBF1* protein expression were increased by pCMV7-*SREBF1c* overexpression. (B) Focus assay of HuH7 cells transfected with control pCMV7 plasmids or pCMV7-*SREBF1c* plasmids. (C) Western blot analysis of *SREBF1* and phospho-GSK-3 β protein expression in HuH7 cells transfected with indicated amounts of pCMV7-*SREBF1c* plasmids.

significance (HR, 3.7; 95% CI, 1.0–13.7; $P = 0.05$; Table 2).

4. Discussion

Using large-scale gene expression profiling, we have shown that the lipogenesis pathway is transcriptionally activated in HCC. Our SAGE profiles will be available on our homepage (<http://www.intmedkanazawa.jp/>) and will be submitted to the Gene Expression Omnibus (<http://www.ncbi.nlm.nih.gov/geo/>).

We found that the levels of expression of *FADS1*, *SCD*, and *FASN* were each correlated with those of

SREBF1, suggesting that *SREBF1* is one of the main factors involved in the activation of lipogenesis in HCC. Activation of growth signaling pathways, such as the PI 3-kinase and mitogen-activated protein kinase pathways, has been shown to induce up-regulation of *SREBF1* in prostate and breast cancer cells [33,34]. We have observed induction of *SREBF1* protein expression by IGF2 in HuH7 cells (data not shown). Furthermore, we have identified that *SREBF1* overexpression results in the activation of cell proliferation and PI 3-kinase signaling, whereas expression inhibition of *SREBF1* abrogated the IGF2 induced cell proliferation. Although detailed mechanisms should be clarified in future, our results suggest that *SREBF1* is a key component of PI 3-kinase signaling in HCC.

SREBF1 is induced by alcohol [35], insulin, and fat [30,36], and plays a central role in the mechanism of hepatic steatosis [37]. Interestingly, these *SREBF1* inducers are risk factors for HCC [12,13,38,14]. Strikingly, two recent studies have shown that HBV and HCV infection may also induce hepatic steatosis through activation of *SREBF1* [39,40]. Furthermore, a recent report revealed the activation of *SREBF1* signaling in cancer by hypoxia [41]. Thus, these pathologic conditions such as chronic viral hepatitis, alcohol abuse, obesity, diabetes, and local hypoxia may up-regulate the expression of *SREBF1*, which, in turn, may contribute to an increased risk of hepatocarcinogenesis. Transgenic mice overexpressing *SREBF1* in the liver exhibited hepatic steatosis and hepatomegaly, suggesting the role of *SREBF1* on lipid metabolism and cell proliferation. However, it should be noted that no transgenic mice overexpressing *SREBF1* have been reported to have the risk of HCC development thus far. Interestingly, a recent report indicated that HCV core transgenic mice known to develop HCC showed coordinated activation of lipogenic pathway genes and *SREBF1* [42]. Although further studies are clearly required, we speculate that the activation of *SREBF1* may contribute to promote the development of HCC in already-initiated hepatocytes but not in normal hepatocytes.

Recently, Yahagi et al. reported the activation of lipogenic enzyme related genes in HCC [31]. In that paper, the authors suggested that *SREBF1* expression was not correlated with the expression of other lipogenic genes by Northern blotting, inconsistent with our current data. One possible explanation of these discrepancies might be the different methods for quantitation of mRNA, and we believe that real-time RT-PCR method used in our study would be more accurate. In addition, we evaluated the expression of *SREBF1* and lipogenic genes using more samples (a total of 44 liver and HCC tissues) than Yahagi et al did (10 HCC tissues). Furthermore, a recent paper indicated the coordinated activation of *SREBF1* and lipogenic genes in HCC

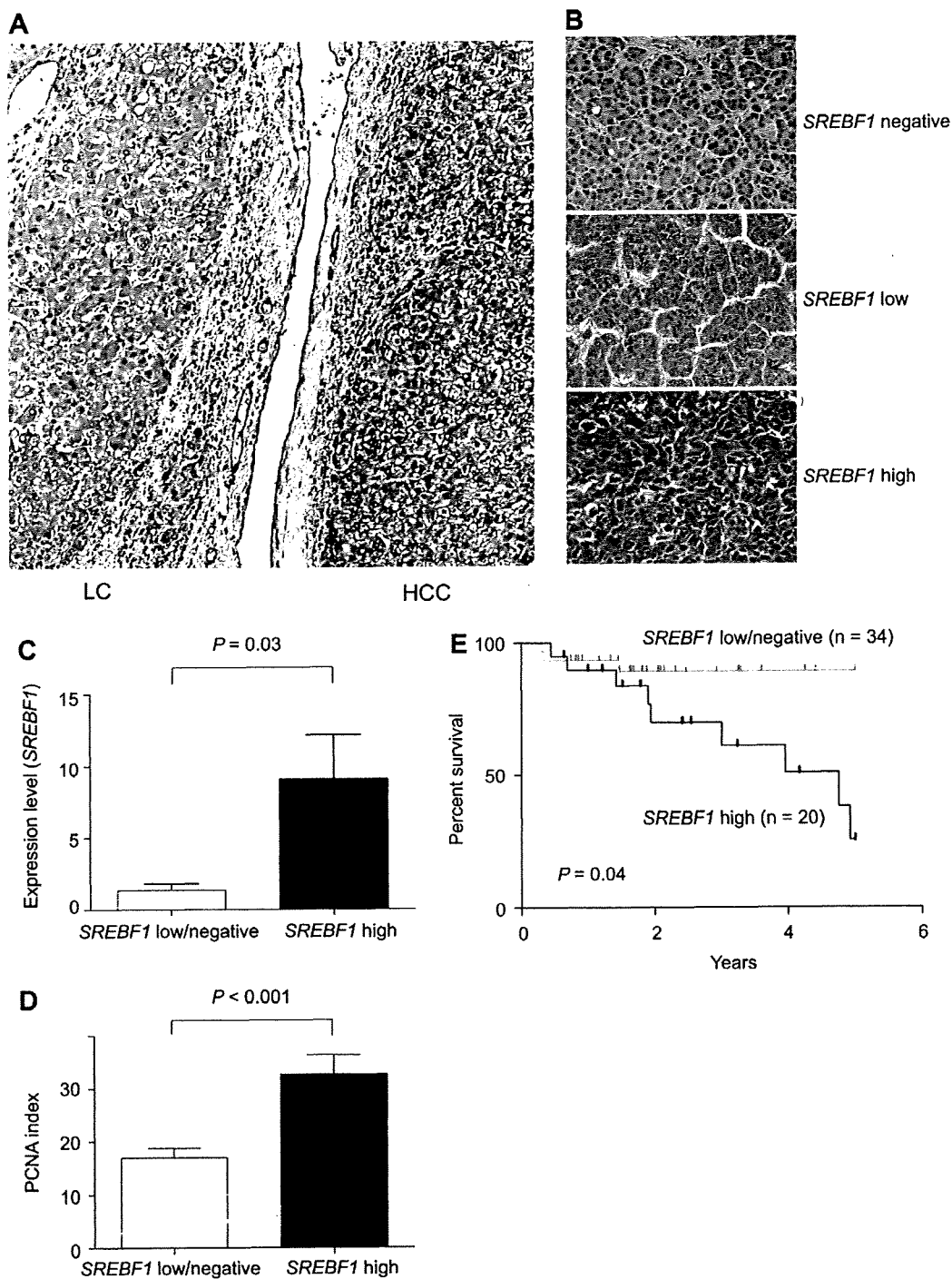


Fig. 4. (A) A photomicrograph of an HCC with adjacent non-cancerous cirrhotic liver stained with anti-*SREBF1* antibodies. (B) Representative photomicrographs of *SREBF1*-negative-, *SREBF1*-low-, and *SREBF1*-high-HCC tissues stained with anti-*SREBF1* antibodies. (C) *SREBF1* gene expression by real-time RT-PCR according to protein expression status assessed by IHC. *SREBF1* was highly expressed in *SREBF1*-high HCC ($P = 0.03$). (D) *SREBF1* expression and cell proliferation in HCC. PCNA indexes in *SREBF1*-high HCC were higher than those in *SREBF1*-low/negative HCC with statistical significance ($P < 0.001$). (E) Kaplan–Meier plots of 54 HCC patients analyzed by immunohistochemistry. The differences between *SREBF1*-high and -low/negative HCC were analyzed by log-rank test.

developed in the liver of HCV core transgenic mice [42], strongly support our data. Although further studies using large numbers of HCC tissues may be required,

these data suggest that the lipogenic gene activation seems to be mediated, at least in part, by *SREBF1* expression in HCC.

Table 2
Univariate Cox regression analysis of survival relative to *SREBF1* protein expression and clinicopathological parameters.

Variables (n)	HR (95% CI)	P-value
<i>SREBF1</i> and mortality (n = 54)		
Tumor size		
<3 cm (n = 37)	1	
≥3 cm (n = 17)	2.2 (0.6–8.3)	0.2
pTNM stage		
I, II (n = 45)	1	
III, IV (n = 9)	2.0 (0.4–9.4)	0.4
Serum AFP		
<20 ng/ml (n = 35)	1	
≥20 ng/ml (n = 19)	1.5 (0.4–5.4)	0.5
<i>SREBF1</i>		
Low (n = 34)	1	
High (n = 20)	3.7 (1.0–13.7)	0.05

Because the majority of our HCC patients analyzed had Child–Pugh class A scores and about 70% had tumors less than 3 cm in diameter, all were expected to have a good prognosis. Indeed, patient survival in this cohort was not segregated by tumor size or pTNM stage (Table 2). Although the sample size was relatively small, we found that enhanced expression of *SREBF1* was a prognostic factor for mortality in HCC possibly due to the highly proliferative nature. Activation of lipogenesis pathways, as shown by overexpression of *FASN*, has been found to correlate with high mortality in breast, prostate, and lung cancer [43], suggesting that activation of lipogenesis may be a fundamental characteristic of cancer with poor prognosis. Thus, *SREBF1* expression may be a good biomarker for HCC classification, a finding that should be validated in a large scale cohort. Because deactivation of the lipogenesis pathway by inhibition of *SREBF1* gene expression could inhibit HCC cell growth *in vitro*, *SREBF1* may be a good target for pharmaceutical intervention in these tumors.

In conclusion, our genome-wide gene expression profiling analyses found that the lipogenesis pathway was activated in a subset of HCC. *SREBF1*, which activates the lipogenesis pathway, may be a good biomarker for HCC prognosis and may be a good target for therapeutic intervention.

Acknowledgements

We are grateful to the members of The Liver Disease Center at Kanazawa University Hospital for providing data of human liver tissue samples. We would also like to thank Dr. Hitoshi Shimano for providing invaluable reagents.

Appendix A. Supplementary data

Supplementary data associated with this article can be found, in the online version, at doi:10.1016/j.jhep.2008.07.036.

References

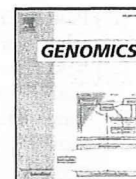
- [1] El-Serag HB, Mason AC. Rising incidence of hepatocellular carcinoma in the United States. *N Engl J Med* 1999;340:745–750.
- [2] Bosch FX, Ribes J, Diaz M, Cleries R. Primary liver cancer: worldwide incidence and trends. *Gastroenterology* 2004;127:S5–S16.
- [3] Wang XW, Hussain SP, Huo TI, Wu CG, Forgues M, Hofseth LJ, et al. Molecular pathogenesis of human hepatocellular carcinoma. *Toxicology* 2002;181–182:43–47.
- [4] Yamashita T, Kaneko S, Hashimoto S, Sato T, Nagai S, Toyoda N, et al. Serial analysis of gene expression in chronic hepatitis C and hepatocellular carcinoma. *Biochem Biophys Res Commun* 2001;282:647–654.
- [5] Shirota Y, Kaneko S, Honda M, Kawai HF, Kobayashi K. Identification of differentially expressed genes in hepatocellular carcinoma with cDNA microarrays. *Hepatology* 2001;33:832–840.
- [6] Okabe H, Satoh S, Kato T, Kitahara O, Yanagawa R, Yamaoka Y, et al. Genome-wide analysis of gene expression in human hepatocellular carcinomas using cDNA microarray: identification of genes involved in viral carcinogenesis and tumor progression. *Cancer Res* 2001;61:2129–2137.
- [7] Xu XR, Huang J, Xu ZG, Qian BZ, Zhu ZD, Yan Q, et al. Insight into hepatocellular carcinogenesis at transcriptome level by comparing gene expression profiles of hepatocellular carcinoma with those of corresponding noncancerous liver. *Proc Natl Acad Sci USA* 2001;98:15089–15094.
- [8] Iizuka N, Oka M, Yamada-Okabe H, Mori N, Tamesa T, Okada T, et al. Comparison of gene expression profiles between hepatitis B virus- and hepatitis C virus-infected hepatocellular carcinoma by oligonucleotide microarray data on the basis of a supervised learning method. *Cancer Res* 2002;62:3939–3944.
- [9] Thorgerisson SS, Grisham JW. Molecular pathogenesis of human hepatocellular carcinoma. *Nat Genet* 2002;31:339–346.
- [10] Lee JS, Thorgerisson SS. Genome-scale profiling of gene expression in hepatocellular carcinoma: classification, survival prediction, and identification of therapeutic targets. *Gastroenterology* 2004;127:S51–S55.
- [11] Surinawinata A, Xu R. An update on the molecular genetics of hepatocellular carcinoma. *Semin Liver Dis* 2004;24:77–88.
- [12] El-Serag HB, Tran T, Everhart JE. Diabetes increases the risk of chronic liver disease and hepatocellular carcinoma. *Gastroenterology* 2004;126:460–468.
- [13] Hassan MM, Hwang LY, Hatten CJ, Swam M, Li D, Abbruzzese JL, et al. Risk factors for hepatocellular carcinoma: synergism of alcohol with viral hepatitis and diabetes mellitus. *Hepatology* 2002;36:1206–1213.
- [14] Ohata K, Hamasaki K, Toriyama K, Matsumoto K, Saeki A, Yanagi K, et al. Hepatic steatosis is a risk factor for hepatocellular carcinoma in patients with chronic hepatitis C virus infection. *Cancer* 2003;97:3036–3043.
- [15] Calle EE, Rodriguez C, Walker-Thurmond K, Thun MJ. Overweight, obesity, and mortality from cancer in a prospectively studied cohort of US adults. *N Engl J Med* 2003;348:1625–1638.
- [16] Walsh MJ, Vanags DM, Clouston AD, Richardson MM, Purdie DM, Jonsson JR, et al. Steatosis and liver cell apoptosis in chronic hepatitis C: a mechanism for increased liver injury. *Hepatology* 2004;39:1230–1238.

- [17] Powell EE, Jonsson JR, Clouston AD. Steatosis: co-factor in other liver diseases. *Hepatology* 2005;42:5–13.
- [18] Velculescu VE, Zhang L, Vogelstein B, Kinzler KW. Serial analysis of gene expression. *Science* 1995;270:484–487.
- [19] Yamashita T, Hashimoto S, Kaneko S, Nagai S, Toyoda N, Suzuki T, et al. Comprehensive gene expression profile of a normal human liver. *Biochem Biophys Res Commun* 2000;269:110–116.
- [20] Desmet VJ, Gerber M, Hoofnagle JH, Manns M, Scheuer PJ. Classification of chronic hepatitis: diagnosis, grading and staging. *Hepatology* 1994;19:1513–1520.
- [21] Polyak K, Xia Y, Zweier JL, Kinzler KW, Vogelstein B. A model for p53-induced apoptosis. *Nature* 1997;389:300–305.
- [22] Yokoyama C, Wang X, Briggs MR, Admon A, Wu J, Hua X, et al. SREBP-1, a basic-helix-loop-helix-leucine zipper protein that controls transcription of the low density lipoprotein receptor gene. *Cell* 1993;75:187–197.
- [23] Wang HC, Chang WT, Chang WW, Wu HC, Huang W, Lei HY, et al. Hepatitis B virus pre-S2 mutant upregulates cyclin A expression and induces nodular proliferation of hepatocytes. *Hepatology* 2005;41:761–770.
- [24] Takeba Y, Kumai T, Matsumoto N, Nakaya S, Tsuzuki Y, Yanagida Y, et al. Irinotecan activates p53 with its active metabolite, resulting in human hepatocellular carcinoma apoptosis. *J Pharmacol Sci* 2007;104:232–242.
- [25] Closset J, Van de Stadt J, Delhaye M, El Nakadi I, Lambilliotte JP, Gelin M. Hepatocellular carcinoma: surgical treatment and prognostic variables in 56 patients. *Hepatogastroenterology* 1999;46:2914–2918.
- [26] Arsura M, Cavin LG, Calvisi DF, Thorgeirsson SS, Eferl R, Ricci R, et al. Nuclear factor-kappaB and liver carcinogenesis. *Cancer Lett* 2005;229:157–169.
- [27] Calvisi DF, Thorgeirsson SS. Molecular mechanisms of hepatocarcinogenesis in transgenic mouse models of liver cancer. *Toxicol Pathol* 2005;33:181–184.
- [28] Eferl R, Ricci R, Kenner L, Zenz R, David JP, Rath M, et al. Liver tumor development. c-Jun antagonizes the proapoptotic activity of p53. *Cell* 2003;112:181–192.
- [29] Xu L, Hui L, Wang S, Gong J, Jin Y, Wang Y, et al. Expression profiling suggested a regulatory role of liver-enriched transcription factors in human hepatocellular carcinoma. *Cancer Res* 2001;61:3176–3181.
- [30] Horton JD, Goldstein JL, Brown MS. SREBPs: activators of the complete program of cholesterol and fatty acid synthesis in the liver. *J Clin Invest* 2002;109:1125–1131.
- [31] Yahagi N, Shimano H, Hasegawa K, Ohashi K, Matsuzaka T, Najima Y, et al. Co-ordinate activation of lipogenic enzymes in hepatocellular carcinoma. *Eur J Cancer* 2005;41:1316–1322.
- [32] Kawaguchi K, Honda M, Yamashita T, Shirota Y, Kaneko S. Differential gene alteration among hepatoma cell lines demonstrated by cDNA microarray-based comparative genomic hybridization. *Biochem Biophys Res Commun* 2005;329:370–380.
- [33] Van de Sande T, De Schrijver E, Heyns W, Verhoeven G, Swinnen JV. Role of the phosphatidylinositol 3'-kinase/PTEN/Akt kinase pathway in the overexpression of fatty acid synthase in LNCaP prostate cancer cells. *Cancer Res* 2002;62:642–646.
- [34] Yang YA, Han WF, Morin PJ, Chrest FJ, Pizer ES. Activation of fatty acid synthesis during neoplastic transformation: role of mitogen-activated protein kinase and phosphatidylinositol 3-kinase. *Exp Cell Res* 2002;279:80–90.
- [35] You M, Fischer M, Deeg MA, Crabb DW. Ethanol induces fatty acid synthesis pathways by activation of sterol regulatory element-binding protein (SREBP). *J Biol Chem* 2002;277:29342–29347.
- [36] Muller-Wieland D, Kotzka J. SREBP-1: gene regulatory key to syndrome X? *Ann NY Acad Sci* 2002;967:19–27.
- [37] Sekiya M, Yahagi N, Matsuzaka T, Najima Y, Nakakuki M, Nagai R, et al. Polyunsaturated fatty acids ameliorate hepatic steatosis in obese mice by SREBP-1 suppression. *Hepatology* 2003;38:1529–1539.
- [38] Marrero JA, Fontana RJ, Su GL, Conjeevaram HS, Emick DM, Lok AS. NAFLD may be a common underlying liver disease in patients with hepatocellular carcinoma in the United States. *Hepatology* 2002;36:1349–1354.
- [39] Kim KH, Shin HJ, Kim K, Choi HM, Rhee SH, Moon HB, et al. Hepatitis B virus X protein induces hepatic steatosis via transcriptional activation of SREBP1 and PPARgamma. *Gastroenterology* 2007;132:1955–1967.
- [40] Wans G, Felmlee DJ, Negro F, Siddiqui A. Hepatitis C virus induces proteolytic cleavage of sterol regulatory element binding proteins and stimulates their phosphorylation via oxidative stress. *J Virol* 2007;81:8122–8130.
- [41] Furuta E, Pai SK, Zhan R, Bandyopadhyay S, Watabe M, Mo YY, et al. Fatty acid synthase gene is up-regulated by hypoxia via activation of Akt and sterol regulatory element binding protein-1. *Cancer Res* 2008;68:1003–1011.
- [42] Tanaka N, Moriya K, Kiyosawa K, Koike K, Gonzalez FJ, Aoyama T. PPARalpha activation is essential for HCV core protein-induced hepatic steatosis and hepatocellular carcinoma in mice. *J Clin Invest* 2008;118:683–694.
- [43] Kuhajda FP. Fatty acid synthase and cancer: new application of an old pathway. *Cancer Res* 2006;66:5977–5980.



ELSEVIER

Genomics

journal homepage: www.elsevier.com/locate/ygeno

Comprehensive gene expression analysis of 5'-end of mRNA identified novel intronic transcripts associated with hepatocellular carcinoma

Yuji Hodo^a, Shin-ichi Hashimoto^b, Masao Honda^a, Taro Yamashita^a, Yutaka Suzuki^c, Sumio Sugano^c, Shuichi Kaneko^{a,*}, Kouji Matsushima^b

^a Department of Gastroenterology, Kanazawa University Graduate School of Medical Science, 13-1 Takara-Machi, Kanazawa, Ishikawa 920-8641, Japan

^b Department of Molecular Preventive Medicine, School of Medicine, The University of Tokyo, 7-3-1, Hongo, Bunkyo-ku, Tokyo 113-0033, Japan

^c Department of Medical Genome Sciences, Graduate School of Frontier Sciences, The University of Tokyo, 5-1-5, Kashwanoha, Kashiwa, Chiba 277-8562, Japan

ARTICLE INFO

Article history:

Received 1 June 2009

Accepted 14 January 2010

Available online xxx

Keywords:

5'-end serial analysis of gene expression

Transcriptional start site

Acyl-coenzyme A oxidase 2

Intron

Hepatocellular carcinoma

ABSTRACT

To elucidate the molecular feature of human hepatocellular carcinoma (HCC), we performed 5'-end serial analysis of gene expression (5'SAGE), which allows genome-wide identification of transcription start sites in addition to quantification of mRNA transcripts. Three 5'SAGE libraries were generated from normal human liver (NL), non-B, non-C HCC tumor (T), and background non-tumor tissues (NT). We obtained 226,834 tags from these libraries and mapped them to the genomic sequences of a total of 8,410 genes using RefSeq database. We identified several novel transcripts specifically expressed in HCC including those mapped to the intronic regions. Among them, we confirmed the transcripts initiated from the introns of a gene encoding acyl-coenzyme A oxidase 2 (ACOX2). The expression of these transcript variants were up-regulated in HCC and showed a different pattern compared with that of ordinary ACOX2 mRNA. The present results indicate that the transcription initiation of a subset of genes may be distinctively altered in HCC, which may suggest the utility of intronic RNAs as surrogate tumor markers.

© 2010 Published by Elsevier Inc.

Introduction

Hepatocellular carcinoma (HCC) is the fifth most common cancer worldwide and the third most common cause of cancer mortality. HCC usually develops in patients with virus-induced (e.g., hepatitis B virus (HBV) and hepatitis C virus (HCV)) chronic inflammatory liver disease [1]; however, non-B, non-C HCC has been reported in patients negative for both HBV and HCV [2]. HCC development is a multistep process involving changes in host gene expression, some of which are correlated with the appearance and progression of a tumor. Multiple studies linking hepatitis viruses and chemical carcinogens with hepatocarcinogenesis have provided insights into tumorigenesis [1,3]. Nevertheless, the genetic events that lead to HCC development remain unknown, and the molecular pathogenesis of HCC in most patients is still unclear. Therefore, elucidation of the genetic changes specific to the pathogenesis of non-B, non-C HCC may be useful to reveal the molecular features of HCCs irrelevant to viral infection.

Gene expression profiling, either by cDNA microarray [4] or serial analysis of gene expression (SAGE) [5], is a powerful molecular technique that allows analysis of the expression of thousands of

genes. In particular, SAGE enables the rapid, quantitative, and simultaneous monitoring of the expression of tens of thousands of genes in various tissues [6,7]. Although numerous studies using cDNA microarrays and SAGE have been performed to clarify the genomic and molecular alterations associated with HCC [6,8-10], most expression data have been derived from the 3'-end region of mRNA. Recent advances in molecular biology have enabled genome-wide analysis of the 5'-end region of mRNA that revealed the variation in transcriptional start sites [11,12] and the presence of a large number of non-coding RNAs [13]. These approaches might be useful for identifying the unique and undefined genes associated with HCC not identified by the analysis of the 3'-end region of mRNA. SAGE based on the 5'-end (5'SAGE), a recently developed technique, allows for a comprehensive analysis of the transcriptional start site and quantitative gene expression [14]. This article is to elucidate the molecular carcinogenesis of non-B, non-C HCCs, while those heterogeneous entities are supposed not to share the same etiology, by using 5'SAGE.

Results

Annotation of the 5'SAGE tags to the human genome

We characterized a total of 226,834 tags from three unique 5'SAGE libraries (75,268 tags from the normal liver (NL) library, 75,573 tags from the non-tumor tissue (NT) library, and 75,993 tags from the tumor (T) library) and compared them against the human genome

Abbreviations: 5'SAGE, 5'-end serial analysis of gene expression; HCC, hepatocellular carcinoma; ACOX2, acyl-coenzyme A oxidase 2.

* Corresponding author. Fax: +81 76 234 4250

E-mail address: skaneko@m-kanazawa.jp (S. Kaneko).

0888-7543/\$ - see front matter © 2010 Published by Elsevier Inc.

doi:10.1016/j.ygeno.2010.01.004

Please cite this article as: Y. Hodo, et al., Comprehensive gene expression analysis of 5'-end of mRNA identified novel intronic transcripts associated with hepatocellular carcinoma, *Genomics* (2010), doi:10.1016/j.ygeno.2010.01.004

81 sequence. A total of 211,818 tags matched genomic sequences, 130
 82 representing 104,820 different tags in the three libraries (Table 1). 131
 83 About 60–65% of these tags mapped to a single locus in the genome in 132
 84 each library. Then, we mapped these single-matched tags to the well- 133
 85 annotated genes using RefSeq database ([www.ncbi.nlm.nih.gov/](http://www.ncbi.nlm.nih.gov/RefSeq/) 134
 86 RefSeq/, reference sequence database developed by NCBI). A total of 135
 87 45,601 tags from the NL library, 39,858 from the NT library, and 136
 88 41,265 from the T library were successfully mapped to 8410 unique 137
 89 genes (4397 genes detected in the NL library, 5194 genes in the NT 138
 90 library, and 6304 genes in the T library).

91 Gene expression profiling of non-B, non-C HCC

92 Abundantly expressed transcripts in the NL library and their 140
 93 corresponding expression in the NT and T libraries are shown in 141
 94 Table 2. The most abundant transcript in all three libraries was 142
 95 encoded by the *albumin* gene. Transcripts encoding apolipoproteins 143
 96 were also abundantly expressed in each library, suggesting the 144
 97 preservation of hepatocytic gene expression patterns in HCC. Of 145
 98 note, the expression of *haptoglobin* (NL: 631, NT: 329, T: 57) and 146
 99 *metallothionein 1G* (NL: 392, NT: 169, T: 2) was decreased in the NT 147
 100 library and more in T library compared with NL library. Furthermore, 148
 101 the expression of *metallothionein 2A* (NL: 1027, NT: 872, T: 19), 149
 102 *metallothionein 1X* (NL: 547, NT: 644, T: 11), and *metallothionein 1E* 150
 103 (NL: 275, NT: 340, T: 2) was decreased almost fifty-fold or more in the 151
 104 T library compared with the NL and NT libraries. In contrast, the 152
 105 expression of *ribosomal protein S29* (NL: 372, NT: 1011, T: 1768) was 153
 106 increased in the NT library and more in T library compared with NL 154
 107 library. Thus, transcripts associated with a certain liver function 155
 108 including xenobiotic metabolism might be suppressed whereas those 156
 109 associated with protein synthesis might be expressed in non-B, non-C 157
 110 HCC, similar to that observed in HCV-HCC [15].

111 We then investigated the characteristics of gene expression 158
 112 patterns in non-B, non C HCC. Two hundred fifty-four and 172 159
 113 genes were up- or down-regulated in the T library more than five-fold 160
 114 compared with the NL library (data not shown). The top 10 genes are 161
 115 listed in Table 3a, and we identified several novel genes not yet 162
 116 reported to be differentially expressed in non-B, non-C HCC. 163
 117 Representative novel gene expression changes identified by 5'SAGE 164
 118 were validated by semi-quantitative reverse transcriptase-polymerase 165
 119 chain reaction (RT-PCR) analysis (Supplemental Fig. 1). RT-PCR 166
 120 results showed that the expression of *galectin 4 (LGALS4)*, *X antigen* 167
 121 *family, member 1 (XAGE 1)*, *retinol dehydrogenase 11 (RDH11)*, *dehydrogenase/reductase member 10 (DHRS10)*, *transmembrane 14A (TMEM14A)*, *stimulated by retinoic acid 13 homolog (STRA13)*, and *dual specificity phosphatase 23 (DUSP23)* was increased, whereas the expression of *C-type lectin superfamily 4 member G (CLEC4G)* was decreased in HCC tissues compared with the non-tumor tissues.

122 To further characterize the gene expression patterns of non-B, 168
 123 non-C HCC comprehensively, we compared the Gene Ontology 169
 124 process of three types of HCCs (i.e., non-B, non-C HCC; HBV-HCC; 170
 125 171
 126 172
 127 173
 128 174
 129 175
 176

HCV-HCC) based on our previously described data [16]. The pathway 130
 analysis using MetaCore™ software showed that the immune related 131
 and cell adhesion related pathways were up-regulated in HCV-HCC 132
 with statistically significance, and the insulin signaling and angio- 133
 genesis related pathways were up-regulated in HBV-HCC with 134
 statistically significance, confirming our previous results [16]. Inter- 135
 estingly, genes associated with progesterone signaling were up- 136
 regulated in non-B, non-C HCC, while genes associated with 137
 proteolysis in the cell cycle, apoptosis and the ESR1-nuclear pathway 138
 were up-regulated in all types of HCC (Supplemental Fig. 2). 139

Dynamic alteration of transcription initiation in HCC

140 Although various transcriptome analyses have discovered consid- 141
 142 erable gene expression changes in cancer, it is still unclear if 143
 transcription is differentially initiated and/or terminated in HCC 144
 compared with the non-cancerous liver. We therefore explored the 145
 characteristics of transcription initiation and/or termination in HCC 146
 using 5'SAGE and 3'SAGE data. Markedly, we observed relevant 147
 differences between 5'SAGE and 3'SAGE data derived from the same 148
 HCC sample (Tables 3a and b). For example, a gene encoding *coagulation factor XIII, B polypeptide* was 13-fold up-regulated at transcription start sites (5'SAGE) but two-fold down-regulated at transcription termination sites (3'SAGE). On the other hand, a gene encoding *adenylate cyclase 1* was 50-fold down-regulated at transcriptional termination sites (3'SAGE) but showed no difference at transcriptional start sites (5'SAGE). These data suggest the dramatic alteration of all process of transcription in HCC, and the transcripts initiated at certain sites might be specifically associated with and involved in HCC pathogenesis, which could be a novel marker for HCC diagnosis. 157

Identification of novel intronic transcripts in HCC

158 Recent lines of evidence suggest that the majority of sequences of 159
 160 eukaryotic genomes may be transcribed, not only from known 161
 transcription start sites but also from intergenic regions and introns 162
 [17,18]. Introns are recognized as a significant source of functional 163
 non-coding RNAs (ncRNAs) including microRNAs (miRNAs) [18]. 164
 Moreover, a recent report implied the role of some large intronic RNAs 165
 in the pathogenesis of several types of malignancies [19]. Thus, 166
 analysis of transcripts originating from introns might be valuable for 167
 elucidating the genetic traits of HCC. We therefore focused on the 168
 transcriptional start sites potentially initiated from the intron and 169
 deregulated in HCC using 5'SAGE data. We identified that 97% of 5' 170
 SAGE tags annotated by the RefSeq database matched the sequences 171
 in the exons, while 3% matched those in the introns (1257 in the N 172
 library, 1225 in the NT library, and 1261 in the T library) (Table 4a). To 173
 identify the possible promoter regions located in the intron, we 174
 clustered the different SAGE tags to a certain genomic region if these 175
 tags positioned within 500 bp intervals (Supplemental Fig. 3), as 176
 described previously [12].

t1.1 **Table 1**
 t1.2 Experimental matching of 5'SAGE tags to genome.

t1.3	Normal liver	Non-tumor	Tumor	Total
t1.4	75,268	75,573	75,993	226,834
t1.5				
t1.6	51,076 (71.2)	47,200 (68.0)	48,503 (68.5)	146,779 (69.3)
t1.7	20,608 (28.8)	22,142 (32.0)	22,289 (31.5)	65,039 (30.7)
t1.8	71,684 (100)	69,342 (100)	70,792 (100)	211,818 (100)
t1.9				
t1.10	20,736 (65.5)	20,487 (60.2)	23,753 (60.7)	64,976 (62.0)
t1.11	10,914 (34.5)	13,548 (39.8)	15,382 (39.3)	39,844 (38.0)
t1.12	31,650 (100)	34,035 (100)	39,135 (100)	104,820 (100)
t1.13	45,601	39,858	41,265	126,724
t1.14	4397	5194	6304	8410

t1.15 5'SAGE indicates 5'-end serial analysis of gene expression.

Please cite this article as: Y. Hodo, et al., Comprehensive gene expression analysis of 5'-end of mRNA identified novel intronic transcripts associated with hepatocellular carcinoma, *Genomics* (2010), doi:10.1016/j.ygeno.2010.01.004

Table 2
The highly expressed genes in the NL library and corresponding expression in the NT and T libraries (top 50 from NL library).

	Tag count			Ratio		Gene
	NL	NT	T	NT/NL	T/NL	
t2.1	3731	1716	2328	0.460	0.624	Albumin
t2.2	2484	2146	2042	0.864	0.822	Apolipoprotein C-I
t2.3	1955	1603	1079	0.820	0.552	Apolipoprotein A-II
t2.4	1653	1050	828	0.635	0.501	Apolipoprotein A-I
t2.5	1252	1908	1203	1.524	0.961	Transthyretin (prealbumin, amyloidosis type I)
t2.6	1233	724	220	0.587	0.178	Serpin peptidase inhibitor, clade A, member 1
t2.7	1027	872	19	0.849	0.019	Metallothionein 2A
t2.8	755	1144	762	1.515	1.009	Ferritin, light polypeptide
t2.9	713	632	680	0.886	0.954	Alpha-1-microglobulin/bikunin precursor
t2.10	635	524	1336	0.825	2.104	Apolipoprotein E
t2.11	631	329	57	0.521	0.090	Haptoglobin
t2.12	600	228	212	0.380	0.353	Fibrinogen gamma chain
t2.13	549	395	302	0.719	0.550	Apolipoprotein C-III
t2.14	547	644	11	1.177	0.020	Metallothionein 1X
t2.15	479	257	290	0.537	0.605	Tumor protein, translationally-controlled 1
t2.16	463	217	53	0.469	0.114	Serpin peptidase inhibitor, clade A, member 3
t2.17	393	204	206	0.519	0.524	Ribosomal protein L26
t2.18	392	169	2	0.431	0.005	Metallothionein 1G
t2.19	372	1011	1768	2.718	4.753	Ribosomal protein S29
t2.20	306	163	223	0.533	0.729	Ribosomal protein S27
t2.21	279	135	159	0.484	0.570	Ribosomal protein S16
t2.22	275	340	2	1.236	0.007	Metallothionein 1E
t2.23	269	170	246	0.632	0.914	Ribosomal protein S23
t2.24	260	142	92	0.546	0.354	Fibrinogen beta chain
t2.25	260	200	195	0.769	0.750	Aldolase B, fructose-bisphosphate
t2.26	255	228	286	0.894	1.122	Ribosomal protein S12
t2.27	248	162	198	0.653	0.798	Ribosomal protein S14
t2.28	246	175	70	0.711	0.285	Interferon induced transmembrane protein 3
t2.29	239	198	273	0.828	1.142	Ribosomal protein L31
t2.30	229	264	0	1.153	0.004	Hepcidin antimicrobial peptide
t2.31	228	149	156	0.654	0.684	Ribosomal protein S20
t2.32	222	191	117	0.860	0.527	Ubiquitin B
t2.33	216	218	352	1.009	1.630	Ribosomal protein L41
t2.34	210	150	155	0.714	0.738	Ribosomal protein, large, P1
t2.35	201	110	90	0.547	0.448	Ribosomal protein, large, P2
t2.36	198	102	64	0.515	0.323	Fibrinogen alpha chain
t2.37	196	143	408	0.730	2.082	Ribosomal protein L37
t2.38	192	123	56	0.641	0.292	Ribosomal protein L37a
t2.39	191	208	346	1.089	1.812	Ribosomal protein L30
t2.40	174	109	76	0.626	0.437	Ribosomal protein L35
t2.41	169	208	3	1.231	0.018	Cytochrome P450, family 2, subfamily E, polypeptide 1
t2.42	167	105	300	0.629	1.796	Apolipoprotein H (beta-2-glycoprotein I)
t2.43	162	106	33	0.654	0.204	Serum amyloid A4, constitutive
t2.44	159	85	157	0.535	0.987	Ribosomal protein L34 (RPL34)
t2.45	159	113	229	0.711	1.440	Transferrin
t2.46	155	84	135	0.542	0.871	Ribosomal protein S11
t2.47	152	125	101	0.822	0.664	Ribosomal protein S13
t2.48	147	84	1	0.571	0.007	Nicotinamide N-methyltransferase
t2.49	147	180	35	1.224	0.238	Hemopexin
t2.50	146	89	121	0.610	0.829	Alpha-2-HS-glycoprotein

To avoid division by 0, a tag value of 1 for any tag that was not detectable was used.
NL, normal liver; NT, non-tumor; T, tumor.

177 More than 2 tags were detected in the intronic regions of the 164
178 genes in the NL, 168 genes in the NT, and 157 genes in the T library,
179 suggesting that these regions might be potential intronic promoter
180 regions (Table 4a). The biological process of these intron-origin
181 transcripts using Human Protein Reference Database (<http://www.hprd.org/>) showed that these were related to basic cellular functions
182 such as signal transduction, transport, and regulation of the
183 nucleobase and nucleotide, suggesting that these intronic transcripts
184 may play a fundamental role in the liver (data not shown). Among
185 these genes, 12 were differentially expressed between the NL and T
186 libraries more than four-fold (Table 4b). Interestingly, intronic
187

Table 3a
Differently expressed genes in HCC (top 10 from 5'SAGE).

5'SAGE	3'SAGE	5'/3'	Gene
T/NL	T/NL	Ratio	
<i>Up-regulated gene</i>			
19	6	3.17	P antigen family, member 2 (prostate associated)
18	10	1.8	Lectin, galactoside-binding, soluble, 4
16	3	5.33	Choline phosphotransferase 1
14	2	7	X antigen family, member 1
14	2	7	Dehydrogenase/reductase (SDR family) member 4
14	2	7	Sterol-C5-desaturase-like
13	0.5	26	Coagulation factor XIII, B polypeptide
13	2.33	5.58	Retinol dehydrogenase 11 (all-trans and 9-cis)
13	0.5	26	Transmembrane protein 14A
12	1.33	9.02	Dual specificity phosphatase 23
<i>Down-regulated gene</i>			
0.00436	0.0137	0.318	Hepcidin antimicrobial peptide
0.0051	ND		Metallothionein 1G
0.0068	0.04	0.17	Nicotinamide N-methyltransferase
0.00727	ND		Metallothionein 1E (functional)
0.0098	0.0526	0.186	C-reactive protein, pentraxin-related
0.0145	ND		Metallothionein 1 M
0.0152	ND		Phospholipase A2, group IIA (platelets, synovial fluid)
0.0178	0.111	0.16	Cytochrome P450, family 2, subfamily E, polypeptide 1
0.0185	0.192	0.096	Metallothionein 2A
0.0201	ND		Metallothionein 1X

3'SAGE, 3'-end serial analysis of gene expression; 5'SAGE, 5'-end serial analysis of gene expression; HCC, hepatocellular carcinoma; NL, normal liver; T, tumor.

transcripts (determined by 5'SAGE) of genes encoding *SAMD3*,
ACO2, *HGD*, *CYP3A5*, *KNG1* and *AGXT* were increased, while their 3'
transcripts (determined by 3'SAGE) were decreased in HCC. In
contrast, both 5' intronic transcripts and 3' transcripts encoding
HFM1, *SERPINA1*, *SUPT3H*, *A2M* and *LR8* were similarly decreased in
HCC. Taken together, these data imply that the canonical- and
intronic-promoter activities of a subset of genes including *SAMD3*,
ACO2, *HGD*, *CYP3A5*, *KNG1* and *AGXT* might be differently regulated
in HCC.

Table 3b
Differently expressed genes in HCC (top 10 from 3'SAGE).

5'SAGE	3'SAGE	5'/3'	Gene
T/NL	T/NL	Ratio	
<i>Up-regulated gene</i>			
ND	15		Leukocyte immunoglobulin-like receptor, subfamily B, member 1
ND	12		Fibroblast growth factor 5
1	11	0.909	Adenosine deaminase, tRNA-specific 1
5	11	0.454	px19-like protein
4.4	11	0.4	APC11 anaphase promoting complex subunit 11 homolog
ND	10.3		Chromosome 21 open reading frame 77
ND	10		von Willebrand factor
2.333	10	0.233	ATX1 antioxidant protein 1 homolog (yeast)
18	10	1.8	Lectin, galactoside-binding, soluble, 4
ND	9.5		Solute carrier family 26 (sulfate transporter), member 2
<i>Down-regulated gene</i>			
0.5	0.012	41.7	ELL associated factor 1
0.5	0.0137	36.5	TGF beta-inducible nuclear protein 1
0.000436	0.0137	0.032	Hepcidin antimicrobial peptide
1	0.0179	55.9	Basic, immunoglobulin-like variable motif containing
ND	0.0182		DNA fragmentation factor, 45 kDa, alpha polypeptide
1	0.0185	54.1	GRIP1 associated protein 1
ND	0.0189		Nuclear factor of activated T-cells 5, tonicity-responsive
1	0.0204	49	Adenylate cyclase 1
0.333	0.0312	10.7	Dihydroorotate dehydrogenase
0.738	0.0312	23.7	Ribosomal protein, large, P1

3'SAGE, 3'-end serial analysis of gene expression; 5'SAGE, 5'-end serial analysis of gene expression; HCC, hepatocellular carcinoma; NL, normal liver; T, tumor.

Please cite this article as: Y. Hodo, et al., Comprehensive gene expression analysis of 5'-end of mRNA identified novel intronic transcripts associated with hepatocellular carcinoma, Genomics (2010), doi:10.1016/j.ygeno.2010.01.004

t5.1 **Table 4a**
t5.2 Number of 5'SAGE tags mapped to intronic region.
t5.3

	NL	NT	T
t5.4 Tag mapped to intron	1287	1253	1292
t5.5 Total promoter region	952	981	1020
t5.6 (tag number = 1)	788	813	863
t5.7 (tag number ≥ 2)	164	168	157

Discussion

227

This is the first comprehensive transcriptional analysis of tissue lesions of non-B, non-C HCC, background liver and NL using the 5' SAGE method. Approximately 6.7% of our 5'SAGE tags showed no matching within the human genome, possibly due to the presence of a single nucleotide polymorphism (SNP) in the human genome. Out of the complete matched tags in the genome, 70% were assigned to unique positions and 30% to two or more loci. The tags with multiple matches with genomic loci were largely retrotransposon elements, repetitive sequences, and pseudogenes.

In this study, the analysis of non-B, non-C HCC enabled us to evaluate direct molecular changes associated with HCC without any bias of gene induction by virus infection. The gene expression profile based on our 5'SAGE tags revealed that albumin and apolipoproteins were highly expressed in NL, indicating the massive production of plasma proteins in NL; these results are similar to those of our previous study using 3'SAGE [6]. Other genes such as *aldolase B*, *antitrypsin*, and *haptoglobin* were also highly expressed in NL, in both the 5'SAGE and 3'SAGE libraries (Table 2) [6]. Comparison of the expression profiles among NL, background NT and T identified several differentially expressed transcripts in T. *Galectin-4* was up-regulated and *hepcidin*, *NNMT*, *CYP2E1*, and *metallothionein* were down-regulated in HCC in accordance with previous findings (Table 3a) [8,9,21]. Moreover, *CLEC4G*, which was predominantly expressed in the sinusoidal endothelial cells of the liver, was down-regulated in HCC. In addition, we first found that *P antigen family, member 2* (*PAGE2*) and *XAGE1* were up-regulated in HCC (Table 3a, Supplemental Fig. 1). These genes were members of cancer-testis antigen that include *MAGE*-family genes. *MAGE*-family members were originally found to be up-regulated in HCV-related HCC, and reported to be useful as molecular markers and as possible target molecules for immunotherapy in human HCC [22]. In this study, we identified that these members of genes were also up-regulated in non B, non-C HCC. Thus, these genes may be useful as molecular markers and therapeutic targets for the treatment of a certain type of human HCC.

There existed some discrepancy between 5'SAGE and 3'SAGE results, even though they were derived from the same sample. Technical issues such as amplification error, difference of restriction enzyme, and annotation error have been described previously [14]. It is possible that 3' transcripts might be more stable than 5' transcripts by binding of ribosomal proteins during translation. Another possibility is the diversity of the transcriptional start and/or termination sites. One of the advantages of 5'SAGE analysis is the potential to determine the transcriptional start sites in each gene. Indeed, a recent study indicated the importance of an insulin splice variant in the pathogenesis of insulinomas [23]. Considering the diversity of 5' ends of genes, it is more appropriate to perform 5'SAGE in combination with 3'SAGE when determining the frequency of gene expression and identifying novel transcript variants.

Here, we were able to identify at least 12 intron-origin transcripts that were differentially expressed in HCC compared with the background liver or NL. These transcripts could not be identified by the 3'SAGE approach. We also performed detailed expression analysis of *ACOX2* that was involved in the beta-oxidation of peroxisome. We were able to clone the intron-origin *ACOX2* RNAs (intrinsic-*ACOX2-1*, 2) for the first time and found that intrinsic-*ACOX2-1* was significantly overexpressed in T compared with NT and NL. The ratio of intrinsic-*ACOX2-1* and canonical *ACOX2* (relative intrinsic-*ACOX2*) was progressively up-regulated from NL via the background liver to HCC. Importantly, the expression of relative intrinsic-*ACOX2* was more up-regulated in moderately differentiated HCC than in well-differentiated HCC. The intronic difference in expression might be due to a polymorphism, since the 5'SAGE library for NL and T were from different people. The mechanisms of stepwise increase of intrinsic-*ACOX2* in the process of hepatocarcinogenesis should be clarified in future.

197 *ACOX2* as a novel intronic gene deregulated in HCC

198 A subset of genes listed above may be transcribed from intronic
199 regions specifically in HCC. Among these genes, we focused on the
200 regulation of *ACOX2*, which is reported to be potentially involved in
201 peroxisomal beta-oxidation and hepatocarcinogenesis [20]. The
202 intron-origin expression of *ACOX2* increased six-fold in HCC
203 compared with the NT by 5'SAGE, while the expression based on
204 the 3' end was almost similar between HCC and NT lesions (Table 4b).
205 Close examination of 5'SAGE data identified two potential intron-
206 origin transcripts of *ACOX2* (Supplemental Fig. 4). The first (intrinsic-
207 *ACOX2-1*) was initiated upstream of the tenth exon, whereas the
208 second (intrinsic-*ACOX2-2*) was initiated upstream of the twelfth
209 exon of *ACOX2* (Supplemental Fig. 4). The sequence of the intronic
210 part was unique, and the remaining part of the sequence was shared
211 with the canonical transcripts of *ACOX2*.

212 The expression of canonical *ACOX2* and the two types of intron-
213 origin transcripts was investigated in NL, NT, and T tissues by RT-PCR
214 (Fig. 1A). Although canonical *ACOX2* expression was decreased in T
215 than in NL, the intron-origin transcript, particularly intrinsic-*ACOX2-1*,
216 was increased in T. Intrinsic-*ACOX2-2* transcripts also showed a
217 modest increase. We further evaluated the alteration of these
218 transcripts in 19 HBV-HCCs, 20 HCV-HCCs, and 4 non-B, non-C
219 HCCs, and their background liver tissues by canonical *ACOX2* and
220 intrinsic-*ACOX2* specific real-time detection (RTD)-PCR. Although the
221 expression of canonical *ACOX2* was decreased, the expression of
222 intrinsic-*ACOX2* was significantly increased (Fig. 1B). Importantly, the
223 gene expression ratios of intrinsic-to canonical *ACOX2* increased more
224 in moderately differentiated HCCs (mHCC) than in well-differentiated
225 HCCs (wHCC), suggesting the involvement of intrinsic-*ACOX2* expres-
226 sion on HCC progression.

t6.1 **Table 4b**
t6.2 Differentially expressed intronic promoter regions in HCC.
t6.3

	5'SAGE T/NL	3'SAGE T/NL	5'/3' Ratio	Gene
t6.4	<i>Up-regulated</i>			
t6.5	9	1	9.00	Sterile alpha motif domain containing 3 (<i>SAMD3</i>)
t6.6	6	0.89	6.74	Acyl-Coenzyme A oxidase 2, branched chain (<i>ACOX2</i>)
t6.7	6	0.62	9.68	Homogentisate 1,2-dioxygenase (homogentisate oxidase) (<i>HGD</i>)
t6.8	6	0.009	666.67	Cytochrome P450, family 3, subfamily A, polypeptide 5 (<i>CYP3A5</i>)
t6.9	5	0.64	7.81	Kininogen 1 (<i>KNG1</i>)
t6.10	4	0.36	11.11	Alanine-glyoxylate aminotransferase (<i>AGXT</i>)
t6.11	4	1	4.00	Crystallin, alpha A (<i>CRYAA</i>)
t6.12	<i>Down-regulated</i>			
t6.13	0.13	1	0.13	HFM1, ATP-dependent DNA helicase homolog (<i>S. cerevisiae</i>) (<i>HFM1</i>)
t6.14	0.25	0.51	0.49	Serpin peptidase inhibitor, clade A member 1 (<i>SERPINA1</i>)
t6.15	0.25	1	0.25	Suppressor of Ty 3 Homolog (<i>S. cerevisiae</i>) (<i>SUPT3H</i>)
t6.16	0.25	0.2	1.25	Alpha-2-macroglobulin (<i>A2M</i>)
t6.17	0.25	0.083	3.13	LR8 protein (<i>LR8</i>)

t6.18 3'SAGE, 3'-end serial analysis of gene expression; 5'SAGE, 5'-end serial analysis of gene expression; HCC, hepatocellular carcinoma; NL, normal liver; NT, non-tumor; T, tumor.

Please cite this article as: Y. Hodo, et al., Comprehensive gene expression analysis of 5'-end of mRNA identified novel intronic transcripts associated with hepatocellular carcinoma, Genomics (2010), doi:10.1016/j.ygeno.2010.01.004

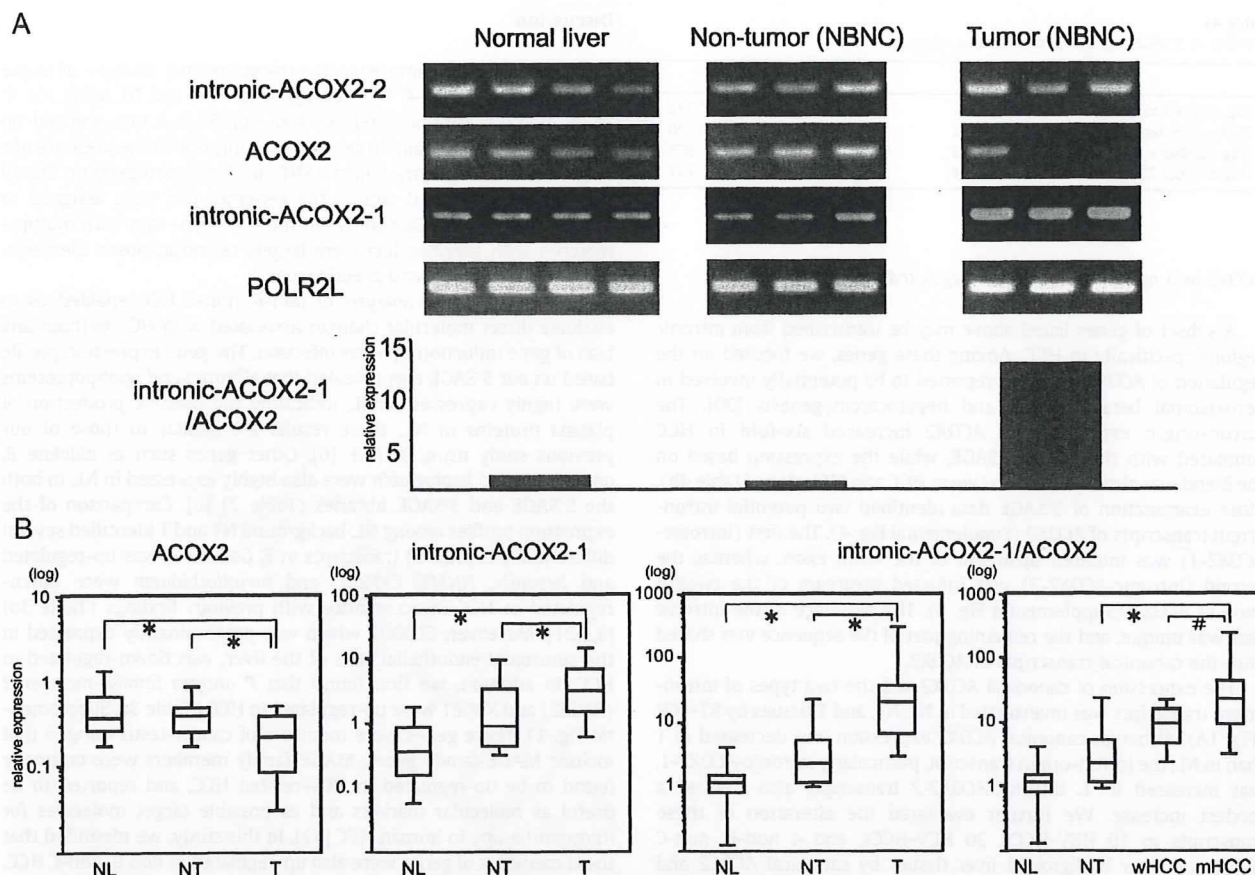


Fig. 1. (A) RT-PCR results of *ACO2* and *ACO2* intronic RNAs in independent NL, NT (non-B, non-C), and T (non-B, non-C) samples. RT-PCR was performed in triplicate for each sample-primer set from cDNA. The PCR products were semi-quantitatively analyzed with ImageJ software and calculated as levels relative to *polymerase (RNA) II (DNA directed) polypeptide L (POLR2L)*. The bar graph indicates the expression ratio of intronic-*ACO2-1* to canonical *ACO2*. The expression pattern of intron 1 was different from that of canonical *ACO2*. (B) RTD-PCR analysis of *ACO2* and *ACO2* intronic RNAs in NL, T (HBV-related, HCV-related, and non-B, non-C), and NT tissues. Quantitative RTD-PCR was performed in duplicate for each sample-primer set from cDNA. Each sample was normalized relative to *POLR2L*. All HCC tissues were pathologically diagnosed as well differentiated HCC (wHCC) or moderately differentiated HCC (mHCC). Kruskal–Wallis tests and Mann–Whitney *U* tests were used for statistical analysis. *ACO2*, acyl-Coenzyme A oxidase 2; HCC, hepatocellular carcinoma; NL, normal liver; NT, non-tumor; RT-PCR, reverse transcriptase-polymerase chain reaction; RTD-PCR, real-time detection-PCR; T, tumor. **P*<0.01, #*P*<0.05.

292 *ACO2* is a rate-limiting enzyme of branched-chain acyl-CoA
 293 oxidase involved in the degradation of long branched fatty acid and
 294 bile acid intermediates in peroxisomes. *ACO2* expression was
 295 associated with the differentiation state of hepatocytes and was
 296 repressed under the undifferentiated phase of human hepatoma cell
 297 lines [24]. A decreased *ACO2* expression was also reported in
 298 prostate cancer [25]. Here, the expression of canonical *ACO2* was
 299 decreased, while that of intronic-*ACO2-1* was increased in HCC. The
 300 deduced amino acid of intronic-*ACO2-1* encodes the C-terminal
 301 (from 386 to 681 amino acids) of canonical *ACO2*, lacking the active
 302 sites for FAD binding and a fatty acid as the substrate, suggesting that
 303 the protein may be functionally departed [26]. The biological role of
 304 the increased intronic-*ACO2-1* was not clear, but it might be
 305 reflected by the activation of peroxisome proliferators-activated
 306 receptor (PPAR). It is reported that mice lacking *ACO1*, another
 307 rate-limiting enzyme in peroxisomal straight-chain fatty acid oxida-
 308 tion, developed steatosis and HCC characterized by increased mRNA
 309 and protein expression of genes regulated by PPAR α [27]. The
 310 importance of PPAR α activation in HCC development has been
 311 recently reported using HCV core protein transgenic mice [28].
 312 Moreover, the overexpression of alpha-methylacyl-CoA racemase,
 313 an enzyme for branched-chain fatty acid beta-oxidation, is reported to
 314 be a reliable diagnostic marker of prostate cancer and is associated

with the decreased expression of *ACO2* [25]. Therefore, the
 expression of intronic-*ACO2-1* might open the door for further
 investigations of their potential clinical use, e.g., serving as diagnostic
 markers of HCC, although the functional relevance of this gene should
 be further clarified.

In conclusion, we report the first comprehensive transcriptional
 analysis of non-B, non-C HCC, NT background liver, and NL tissue,
 based on 5'SAGE. This study offers new insights into the transcrip-
 tional changes that occur during HCC development as well as the
 molecular mechanism of carcinogenesis in the liver. The results
 suggest the presence of unique intron-origin RNAs that are useful as
 diagnostic markers and may be used as new therapeutic targets.

Material and methods

Samples

Samples were obtained from a 56-year-old man who had
 undergone surgical hepatic resection for the treatment of solitary
 HCC. Serological tests for hepatitis B surface (HBs) antigen and anti-
 HCV antibodies were negative. Tumor (T) and non-tumor (NT) tissue
 samples were separately obtained from the tumorous parts (diag-
 nosed as moderately differentiated HCC) and non-tumorous parts

(diagnosed as mild chronic hepatitis: F1A1) of the resected tissue. We also obtained five normal liver (NL) tissue samples from five patients who had undergone surgical hepatic resection because of metastatic liver cancer. None of the patients was seropositive for both HBs antigen and anti-HCV antibodies. Neither heavy alcohol consumption nor the intake of chemical agents was observed before surgical resection. All laboratory values related to hepatic function were within the normal range. All procedures and risks were explained verbally and provided in a written consent form.

We additionally used independent four NL tissue samples, 19 HBV-HCCs, 20 HCV-HCCs and 4 non-B, non-C HCCs, and their background liver tissue samples for reverse transcriptase-polymerase chain reaction (RT-PCR) and real-time detection (RTD)-PCR (Supplemental Table 1). Four non-B, non-C HCCs were histologically diagnosed as moderately differentiated HCCs, and the adjacent non-cancerous liver tissues were diagnosed as a normal liver, a chronic hepatitis, a pre-cirrhotic liver and a cryptogenic liver cirrhosis, respectively. None of the patients was seropositive for HBs antigen, anti-HBs antibodies, anti-hepatitis B core (HBC) antibodies and anti-HCV antibodies. Neither heavy alcohol consumption nor the intake of chemical agents was observed. Histological grading of the tumor was evaluated by two independent pathologists as described previously [16].

357 Generation of the 5' SAGE library

5'SAGE libraries were generated as previously described [14]. Five to ten micrograms of poly(A)+RNA was treated with bacterial alkaline phosphatase (BAP; TaKaRa, Otsu, Japan). Poly(A)+RNA was extracted twice with phenol: chloroform (1:1), ethanol precipitated, and then treated with tobacco acid pyrophosphatase (TAP). Two to four micrograms of the BAP-TAP-treated poly(A)+RNA was divided into two aliquots and an RNA linker containing recognition sites for *EcoRI/MmeI* was ligated using RNA ligase (TaKaRa): one aliquot was ligated to a 5'-oligo 1 (5'-GGA UUU GCU GGU GCA GUA CAA CGA AUU CCG AC-3') linker, and the other aliquot was ligated to a 5'-oligo 2 (5'-CUG CUC GAA UGC AAG CUU CUG AAU UCC GAC-3') linker. After removing unligated 5'-oligo, cDNA was synthesized using RNaseH-free reverse-transcriptase (Superscript II, Invitrogen, Carlsbad, CA, USA) at 12 °C for 1 h and 42 °C for the next hour, using 10 pmol of dT adapter-primer (5'-GCG GCT GAA GAC GGC CTA TGT GGC CTT TTT TTT TTT TTT-3'). After first-strand synthesis, RNA was degraded in 15 mM NaOH at 65 °C for 1 h. cDNA was amplified in a volume of 100 µl by PCR with 16 pmol of 5' (5'-[biotin]-GGA TTT GCT GGT GCA GTA CAA-3' or 5'-[biotin]-CTG CTC GAA TGC AAG CIT CTG-3') and 3' (5'-GCG GCT GAA GAC GGC CTA TGT-3') PCR primers. cDNA was amplified using 10 cycles at 94 °C for 1 min, 58 °C for 1 min, and 72 °C for 2 min. PCR products were digested with the *MmeI* type IIS restriction endonuclease (NEB, Pickering, Ontario, Canada). The digested 5'-terminal cDNA fragments were bound to streptavidin-coated magnetic beads (DynaL, Oslo, Norway). cDNA fragments that bound to the beads were directly ligated together in a reaction mixture containing T4 DNA ligase in a supplied buffer for 2.5 h at 16 °C. The ditags were amplified by PCR using the following primers: 5' GGA TTT GCT GGT GCA GTA CA 3' and 5' CTG CTC GAA TGC AAG CTT CT 3'. The PCR products were analyzed by polyacrylamide gel electrophoresis (PAGE) and digested with *EcoRI*. The region of the gel containing the ditags was excised and the fragments were self-ligated to produce long concatamers that were then cloned into the *EcoRI* site of pZero 1.0 (Invitrogen). Colonies were screened by PCR using the M13 forward and reverse primers. PCR products containing inserts of more than 600 bp were sequenced with Big Dye terminator ver.3 and analyzed using a 3730 ABI automated DNA sequencer (Applied Biosystems, Foster City, CA, USA). All electrophoretograms were reanalyzed by visual inspection to check for ambiguous bases and to correct misreads. In this study, we obtained 19–20 bp tag information.

Association of the 5'SAGE tags with their corresponding genes

399

We attempted to align our 5'tags with the human genome (NCBI build 36, available from <http://www.genome.ucsc.edu/>) using the alignment program ALPS (<http://www.alps.gi.k.u-tokyo.ac.jp/>). Only tags that matched in sense orientation were considered in our analysis. The RefSeq database was searched for transcripts corresponding to the regions adjacent to the alignment location of each 5'tag.

RT-PCR

407

Total RNA was extracted using a ToTally RNA extraction kit (Ambion, Inc., Austin, TX, USA). Total RNA (500 ng) was reverse-transcribed in a 100-µl reaction solution containing 240 U of Moloney murine leukemia virus reverse transcriptase (Promega, Madison, WI, USA), 80 U of RNase inhibitor (Promega), 4.6 mM MgCl₂, 6.6 mM DTT, 1 mM dNTPs, and 2 mM random hexamer (Promega), at 42 °C for 1 h. PCR was performed in a 20-µl volume containing 0.5 U of AmpliTaq DNA polymerase (Applied Biosystems), 16.6 mM (NH₄)₂SO₄, 67 mM Tris-HCl, 6.7 mM MgCl₂, 10 mM 2-mercaptoethanol, 1 mM dNTPs, and 1.5 µM sense and antisense primers, using an ABI 9600 thermal cycler (Applied Biosystems). The amplification protocol included 28–30 cycles of 95 °C for 45 s, 58 °C for 1 min, and 72 °C for 1 min. Primer sequences are shown in Supplemental Table 2. RT-PCR was performed in triplicate for each sample-primer set. Each sample was normalized relative to *polymerase (RNA) II (DNA directed) polypeptide L (POLR2L)*. *POLR2L* is a housekeeping gene that showed relatively stable gene expression in various tissues [29]. The PCR products were semi-quantitatively analyzed with ImageJ software (<http://rsb.info.nih.gov/ij/>).

RTD-PCR

427

Intron-origin transcript expression was quantified using TaqMan Universal Master Mix (Applied Biosystems). The samples were amplified using an ABI PRISM 7900HT Sequence Detection System (Applied Biosystems). Using the standard curve methods, quantitative PCR was performed in duplicate for each sample-primer set. Each sample was normalized relative to *POLR2L*. The assay IDs used were Hs00185873_m1 for *ACOX2* and Hs00360764_m1 for *POLR2L*. The specific primers and probe sequence of intronic-*ACOX2-1* were 5'-TTCATAAAGTTGTGAGCAGAGGAAA-3' (forward), 5'-TGCACCACITACT-GAGCATCTACTC-3' (reverse), and 5'-ACTTCTTACTCAGAGCTG-3' (probe).

Analysis of pathway network

439

MetaCore™ software (GeneGo Inc., St. Joseph, MI) was used to investigate the molecular pathway networks of non-B, non-C HCC, HBV-HCC and HCV-HCC. All genes up-regulated more than five-fold in all HCC libraries subjected to Enrichment analysis in GO process networks by default settings (p<0.05).

Statistical analysis

445

Kruskal-Wallis tests were used to compare the expression among normal liver, non-cancerous tissues, and HCC tissues. Mann-Whitney *U* tests were also used to evaluate the statistical significance of *ACOX2* gene expression levels between two groups. All statistical analyses were performed using R (<http://www.r-project.org/>).

Acknowledgments

451

The authors would like to thank Mr. Shungo Deshimaru and Ms. Keiko Harukawa for technical assistance.

452

453

Please cite this article as: Y. Hodo, et al., Comprehensive gene expression analysis of 5'-end of mRNA identified novel intronic transcripts associated with hepatocellular carcinoma, *Genomics* (2010), doi:10.1016/j.ygeno.2010.01.004

454 **Appendix A. Supplementary data**

455 Supplementary data associated with this article can be found, in
456 the online version, at doi:10.1016/j.ygeno.2010.01.004.

457 **References**

- 458 [1] H.B. El-Serag, K.L. Rudolph, Hepatocellular carcinoma: epidemiology and
459 molecular carcinogenesis, *Gastroenterology* 132 (2007) 2557–2576.
- 460 [2] Y. Yokoi, S. Suzuki, S. Baba, K. Inaba, H. Konno, S. Nakamura, Clinicopathological
461 features of hepatocellular carcinomas (HCCs) arising in patients without chronic
462 viral infection or alcohol abuse: a retrospective study of patients undergoing
463 hepatic resection, *J. Gastroenterol.* 40 (2005) 274–282.
- 464 [3] R.N. Aravalli, C.J. Steer, E.N. Cressman, Molecular mechanisms of hepatocellular
465 carcinoma, *Hepatology* 48 (2008) 2047–2063.
- 466 [4] D.J. Duggan, M. Bittner, Y. Chen, P. Meltzer, J.M. Trent, Expression profiling using
467 cDNA microarrays, *Nat. Genet.* 21 (1999) 10–14.
- 468 [5] V.E. Velculescu, L. Zhang, B. Vogelstein, K.W. Kinzler, Serial analysis of gene
469 expression, *Science* 270 (1995) 484–487.
- 470 [6] T. Yamashita, S. Hashimoto, S. Kaneko, S. Nagai, N. Toyoda, T. Suzuki, K. Kobayashi,
471 K. Matsushima, Comprehensive gene expression profile of a normal human liver,
472 *Biochem. Biophys. Res. Commun.* 269 (2000) 110–116.
- 473 [7] S. Hashimoto, S. Nagai, J. Sese, T. Suzuki, A. Obata, T. Sato, N. Toyoda, H.Y. Dong, M.
474 Kurachi, T. Nagahata, K. Shizuno, S. Morishita, K. Matsushima, Gene expression
475 profile in human leukocytes, *Blood* 101 (2003) 3509–3513.
- 476 [8] H. Okabe, S. Satoh, T. Kato, O. Kitahara, R. Yanagawa, Y. Yamaoka, T. Tsunoda, Y.
477 Furukawa, Y. Nakamura, Genome-wide analysis of gene expression in human
478 hepatocellular carcinomas using cDNA microarray: identification of genes
479 involved in viral carcinogenesis and tumor progression, *Cancer. Res.* 61 (2001)
480 2129–2137.
- 481 [9] Y. Shirota, S. Kaneko, M. Honda, H.F. Kawai, K. Kobayashi, Identification
482 of differentially expressed genes in hepatocellular carcinoma with cDNA
483 microarrays, *Hepatology* 33 (2001) 832–840.
- 484 [10] T. Yamashita, M. Honda, S. Kaneko, Application of serial analysis of gene
485 expression in cancer research, *Curr. Pharm. Biotechnol.* 9 (2008) 375–382.
- 486 [11] Y. Suzuki, H. Taira, T. Tsunoda, J. Mizushima-Sugano, J. Sese, H. Hata, T. Ota, T.
487 Isogai, T. Tanaka, S. Morishita, K. Okubo, Y. Sakaki, Y. Nakamura, A. Suyama, S.
488 Sugano, Diverse transcriptional initiation revealed by fine, large-scale mapping of
489 mRNA start sites, *EMBO Rep.* 2 (2001) 388–393.
- 490 [12] K. Kimura, A. Wakamatsu, Y. Suzuki, T. Ota, T. Nishikawa, R. Yamashita, J.
491 Yamamoto, M. Sekine, K. Tsuritani, H. Wakaguri, S. Ishii, T. Sugiyama, K. Saito, Y.
492 Isono, R. Irie, N. Kushida, T. Yoneyama, R. Otsuka, K. Kanda, T. Yokoi, H. Kondo, M.
493 Wagatsuma, K. Murakawa, S. Ishida, T. Ishibashi, A. Takahashi-Fujii, T. Tanase, K.
494 Nagai, H. Kikuchi, K. Nakai, T. Isogai, S. Sugano, Diversification of transcriptional
495 modulation: large-scale identification and characterization of putative alternative
496 promoters of human genes, *Genome. Res.* 16 (2006) 55–65.
- 497 [13] T. Shiraki, S. Kondo, S. Katayama, K. Waki, T. Kasukawa, H. Kawaji, R. Rodzius, A.
498 Watahiki, M. Nakamura, T. Arakawa, S. Fukuda, D. Sasaki, A. Podhajsky, M.
499 Harbers, J. Kawai, P. Carninci, Y. Hayashizaki, Cap analysis gene expression for
500 high-throughput analysis of transcriptional starting point and identification of
501 promoter usage, *Proc. Natl. Acad. Sci. U. S. A.* 100 (2003) 15776–15781.
- [14] S. Hashimoto, Y. Suzuki, Y. Kasai, K. Morohoshi, T. Yamada, J. Sese, S. Morishita, S. Sugano, K. Matsushima, 5'-end SAGE for the analysis of transcriptional start sites, *Nat. Biotechnol.* 22 (2004) 1146–1149.
- [15] T. Yamashita, S. Kaneko, S. Hashimoto, T. Sato, S. Nagai, N. Toyoda, T. Suzuki, K. Kobayashi, K. Matsushima, Serial analysis of gene expression in chronic hepatitis C and hepatocellular carcinoma, *Biochem. Biophys. Res. Commun.* 282 (2001) 647–654.
- [16] T. Yamashita, M. Honda, H. Takatori, R. Nishino, H. Minato, H. Takamura, T. Ohta, S. Kaneko, Activation of lipogenic pathway correlates with cell proliferation and poor prognosis in hepatocellular carcinoma, *J. Hepatol.* 50 (2009) 100–110.
- [17] J.S. Mattick, Introns: evolution and function, *Curr. Opin. Genet. Dev.* 4 (1994) 823–831.
- [18] J.S. Mattick, I.V. Makunin, Non-coding RNA, *Hum. Mol. Genet.* 15 (Spec No 1) (2006) R17–29.
- [19] R. Louro, A.S. Smirnova, S. Verjovskj-Almeida, Long intronic noncoding RNA transcription: expression noise or expression choice? *Genomics* 93 (2009) 291–298.
- [20] S. Yu, S. Rao, J.K. Reddy, Peroxisome proliferator-activated receptors, fatty acid oxidation, steatohepatitis and hepatocarcinogenesis, *Curr. Mol. Med.* 3 (2003) 561–572.
- [21] N. Kondoh, T. Wakatsuki, A. Ryo, A. Hada, T. Aihara, S. Horuchi, N. Goseki, O. Matsubara, K. Takenaka, M. Shichita, K. Tanaka, M. Shuda, M. Yamamoto, Identification and characterization of genes associated with human hepatocellular carcinogenesis, *Cancer. Res.* 59 (1999) 4990–4996.
- [22] Y. Kobayashi, T. Higashi, K. Nouse, H. Nakatsukasa, M. Ishizaki, T. Kaneyoshi, N. Toshihumi, K. Kariyama, E. Nakayama, T. Tsuji, Expression of MAGE, GAGE and BAGE genes in human liver diseases: utility as molecular markers for hepatocellular carcinoma, *J. Hepatol.* 32 (2000) 612–617.
- [23] A.H. Minn, M. Kayton, D. Lorang, S.C. Hoffmann, D.M. Harlan, S.K. Libutti, A. Shalev, Insulinomas and expression of an insulin splice variant, *Lancet* 363 (2004) 363–367.
- [24] H. Stier, H.D. Fahimi, P.P. Van Veldhoven, G.P. Mannaerts, A. Volk, E. Baumgart, Maturation of peroxisomes in differentiating human hepatoblastoma cells (HepG2): possible involvement of the peroxisome proliferator-activated receptor alpha (PPAR alpha), *Differentiation* 64 (1998) 55–66.
- [25] S. Zha, S. Ferdinandusse, J.L. Hicks, S. Denis, T.A. Dunn, R.J. Wanders, J. Luo, A.M. De Marzo, W.B. Isaacs, Peroxisomal branched chain fatty acid beta-oxidation pathway is upregulated in prostate cancer, *Prostate* 63 (2005) 316–323.
- [26] K. Tokuoka, Y. Nakajima, K. Hirotsu, I. Miyahara, Y. Nishina, K. Shiga, H. Tamaoki, C. Setoyama, H. Tojo, R. Miura, Three-dimensional structure of rat-liver acyl-CoA oxidase in complex with a fatty acid: insights into substrate-recognition and reactivity toward molecular oxygen, *J. Biochem.* 139 (2006) 789–795.
- [27] K. Meyer, Y. Jia, W.Q. Cao, P. Kashreddy, M.S. Rao, Expression of peroxisome proliferator-activated receptor alpha, and PPARalpha regulated genes in spontaneously developed hepatocellular carcinomas in fatty acyl-CoA oxidase null mice, *Int. J. Oncol.* 21 (2002) 1175–1180.
- [28] N. Tanaka, K. Moriya, K. Kiyosawa, K. Koike, F.J. Gonzalez, T. Aoyama, PPARalpha activation is essential for HCV core protein-induced hepatic steatosis and hepatocellular carcinoma in mice, *J. Clin. Invest.* 118 (2008) 683–694.
- [29] C. Rubie, K. Kempf, J. Hans, T. Su, B. Tilton, T. Georg, B. Brittner, B. Ludwig, M. Schilling, Housekeeping gene variability in normal and cancerous colorectal, pancreatic, esophageal, gastric and hepatic tissues, *Mol. Cell. Probes.* 19 (2005) 101–109.

CLINICAL STUDIES

dUTP pyrophosphatase expression correlates with a poor prognosis in hepatocellular carcinoma

Hajime Takatori¹, Taro Yamashita¹, Masao Honda¹, Ryuhei Nishino¹, Kuniaki Arai¹, Tatsuya Yamashita¹, Hiroyuki Takamura², Tetsuo Ohta², Yoh Zen³ and Shuichi Kaneko¹

1 Department of Gastroenterology, Kanazawa University Graduate School of Medical Science, Ishikawa, Japan

2 Department of Gastroenterologic Surgery, Kanazawa University Graduate School of Medical Science, Ishikawa, Japan

3 Pathology Section, Kanazawa University Hospital, Ishikawa, Japan

Keywords

dUTP pyrophosphatase – hepatocellular carcinoma – prognosis – serial analysis of gene expression

Abbreviations

5-FU, 5-fluorouracil; dUTPase, dUTP pyrophosphatase; HCC, hepatocellular carcinoma; IHC, immunohistochemistry; qRT-PCR, quantitative reverse transcription-polymerase chain reaction; SAGE, serial analysis of gene expression.

Correspondence

Masao Honda, MD, Department of Gastroenterology, Kanazawa University Graduate School of Medical Science, 13-1 Takara-Machi, Kanazawa, Ishikawa 920-8641, Japan
Tel: +81 76 265 2233
Fax: +81 76 234 4250
e-mail: mhonda@m-kanazawa.jp

Received 13 August 2009

Accepted 26 October 2009

DOI:10.1111/j.1478-3231.2009.02177.x

Abstract

Background: Hepatocellular carcinoma (HCC) is a malignancy with a poor prognosis, partly owing to the lack of biomarkers that support its classification in line with its malignant nature. To discover a novel molecular marker that is related to the efficacy of treatment for HCC and its biological nature, we performed serial analysis of gene expression (SAGE) in HCC, normal liver and cirrhotic liver tissues. **Methods:** Gene expression profiles of HCC tissues and non-cancerous liver tissues were obtained by SAGE. Suppression of the target gene by RNA interference was used to evaluate its role in HCC *in vitro*. The relation of the identified marker and prognosis was statistically examined in surgically resected HCC patients. **Results:** We identified significant over-expression of *DUT*, which encodes dUTP pyrophosphatase (dUTPase), in HCC tissue, and this was confirmed in about two-thirds of the HCC samples by reverse-transcription polymerase chain reaction ($n = 20$). Suppression of dUTPase expression using short interfering RNAs inhibited cell proliferation and sensitized HuH7 cells to 5-fluorouracil treatment. Nuclear dUTPase expression was observed in 36.6% of surgically resected HCC samples ($n = 82$) evaluated by immunohistochemistry, and its expression was significantly correlated with the histological grades ($P = 0.0099$). Notably, nuclear dUTPase expression correlated with a poor prognosis with statistical significance (HR, 2.47; 95% CI, 1.08–5.66; $P = 0.032$). **Conclusion:** Taken together, these results suggest that nuclear dUTPase may be a good biomarker for predicting prognosis in HCC patients after surgical resection. Development of novel dUTPase inhibitors may facilitate the eradication of HCC.

Hepatocellular carcinoma (HCC) is the fifth most common malignancy and the third leading cause of cancer-related death worldwide (1). Several risk factors are responsible for HCC development, including alcoholism, aflatoxin and genetic diseases such as haemochromatosis and α -1 antitrypsin deficiency; however, the major risk factor is chronic hepatitis owing to hepatitis B virus (HBV) or hepatitis C virus (HCV) infection (2–4). Several treatment options are currently available for HCC management, which include liver transplantation, surgical resection, percutaneous ethanol injection, radio-frequency ablation, transcatheter arterial chemoembolization and systemic or local chemotherapy, and optimal treatment is determined based on tumour stage and liver function (5, 6). However, more than 80% of HCC cases develop advanced HCC after initial treatment (7).

Various chemotherapeutic drugs have been investigated for their antitumour activity in advanced HCC. For example, 5-fluorouracil (5-FU), a thymidylate synthase inhibitor, was the first reported drug studied for the treatment of advanced HCC; however, a median survival rate of 3–5 months has discouraged the further use of 5-FU as a single chemotherapeutic agent (8, 9). Interferon- α (IFN- α) has been reported to have antitumour activity against advanced HCC, and recent reports have suggested the efficacy of a combination of 5-FU/IFN- α for advanced HCC treatment (10–12), although convincing evidence for improved survival rate remains lacking. A recent study has indicated that 16% of advanced HCC patients responded positively to 5-FU/IFN- α treatment with clear and significant survival benefits compared with stable or progressive disease

patients (13). Thus, drug sensitivity appears to be one of the major determinants of the prognosis of advanced HCC patients treated with chemotherapy. Therefore, a hallmark of successful treatment would be the identification of useful biomarkers for determining the survival benefits offered by each treatment strategy.

In this study, we investigated the gene expression profiles of HCCs using serial analysis of gene expression (SAGE) to identify novel molecular markers or targets for the treatment of HCC (14–18). Here, we identified the upregulation of the *DUT* gene that encodes dUTP pyrophosphatase (dUTPase) in HCC. Markedly, HCC with a high nuclear dUTPase expression correlated with a poorly differentiated morphology and a poor prognosis. *DUT* gene knockdown not only suppressed cell proliferation but also sensitized HuH7 cells to low-dose 5-FU.

Materials and methods

Samples

All HCC tissues, adjacent non-cancerous liver tissues and normal liver tissues were obtained from 110 patients undergoing a hepatectomy between 1997 and 2006 in Kanazawa University Hospital, Kanazawa, Japan. Five normal liver tissue samples were obtained from patients undergoing surgical resection of the liver for the treatment of metastatic colon cancer. These samples were snap-frozen in liquid nitrogen immediately after resection. One hundred and five HCC and surrounding non-cancerous liver samples were obtained from patients undergoing surgical resection of the liver for HCC treatment, and part of these samples were used for the recent study (19). Three HCC and adjacent non-cancerous liver tissue samples were snap-frozen in liquid nitrogen and later used for SAGE. Twenty HCC tissues and their corresponding non-cancerous liver tissues were also snap-frozen and later used for real-time reverse transcription-polymerase chain reaction (RT-PCR) analysis, as described previously (19). Eighty-two additional HCC samples were formalin-fixed, paraffin-embedded and used for immunohistochemistry (IHC). HCC and adjacent non-cancerous liver tissues were histologically characterized, as reported elsewhere (19).

All strategies used for gene expression analysis as well as tissue acquisition processes were approved by the Ethics Committee and the Institutional Review Board of Kanazawa University Hospital. All procedures and risks were explained verbally to each patient, who then provided written informed consent.

Serial analysis of gene expression

Total RNA was purified from each homogenized tissue sample using a ToTally RNA extraction kit (Ambion Inc., Austin, TX, USA), and polyadenylated RNA was isolated using a MicroPoly (A) Pure kit (Ambion). A total of 2.5 µg of mRNA per sample was analysed by SAGE (20, 21). SAGE libraries were randomly sequenced at the

Genomic Research Center (Shimadzu-Biotechnology, Kyoto, Japan), and the sequence files were analysed with SAGE 2000 software. The size of each SAGE library was normalized to 300 000 transcripts per library, and the abundance of transcripts was compared with SAGE 2000 software. Monte Carlo simulation was used for selecting genes whose expression levels were significantly different between the two libraries (22). Each SAGE tag was annotated using a gene-mapping website SAGE Genie database (<http://cgap.nci.nih.gov/SAGE/>) and the Source database (<http://smd.stanford.edu/cgi-bin/source/sourceSearch>), as described previously (23).

Quantitative reverse transcription-polymerase chain reaction

A 1 µg aliquot of each total RNA was reverse-transcribed using SuperScript II reverse-transcriptase (Invitrogen, Carlsbad, CA, USA). Real-time RT-PCR analysis was performed using the ABI PRISM 7700 sequence detection system (Applied Biosystems, Foster City, CA, USA). Using the standard curve method, quantitative PCR was performed in duplicate for each sample-primer set. Each sample was normalized relative to β actin. The assay IDs used were Hs00798995_s1 for dUTPase and Hs99999903_m1 for β actin.

RNA interference targeting *DUT*

Small interfering RNAs (siRNAs) targeting *DUT* or control (scrambled sequence) were synthesized by Dharmacon (Dharmacon Research Inc., Lafayette, CO, USA). The target sequences of *DUT* are 5'-AAGUUGU GAAAACGGACAUC-3' (*DUT*1) and 5'-CGGACAUC CAGAUAGCGCUTT-3' (*DUT*2). Lipofectamine 2000™ reagent (Invitrogen) was used for transfection according to the manufacturer's instructions.

Cell proliferation assay, soft agar assay and matrigel invasion assay

Cell proliferation assays were performed using a Cell Titer96 Aqueous kit in quintuplicate (Promega, Madison, WI, USA). For the soft agar assay, 1×10^4 cells were suspended in 2 ml of 0.36% agar with growth medium and added in each well of a six-well plate containing a base layer of 0.72% agar. The plates were incubated at 37 °C in a 5% CO₂ incubator for 2 weeks. Matrigel invasion assays were performed using BD BioCoat™ Matrigel Matrix Cell Culture Inserts and Control Inserts (BD Biosciences, San Jose, CA, USA), as described in the manufacturer's instruction. 5-FU was obtained from Kyowa Kirin (Kyowa Kirin, Tokyo, Japan). All experiments were repeated at least twice.

Immunohistochemistry

Mouse monoclonal anti-dUTPase antibody M01 (Abnova Corporation, Taipei, Taiwan) and mouse antiproliferating

cell nuclear antigen (PCNA) monoclonal antibody PC10 (Calbiochem, San Diego, CA, USA) were used to evaluate the immunoreactivity of HCC and adjacent non-cancerous liver samples using a Dako EnVision+™ kit (Dako, Carpinteria, CA, USA), according to the manufacturer's instruction. Immunoreactivity was evaluated by determining the percentage of cells expressing dUTPase in the examined fields, graded as low (0–50%) or high (> 50%). The PCNA index was evaluated as described previously (19).

Statistical analysis

Student's *t*-test was used to determine the statistical significance of the differences in cell viability between the two groups. The Mann–Whitney *U*-test was used for the analysis of gene expression between chronic liver disease (CLD) and HCC tissues. The χ^2 -test was used to evaluate the correlation between clinicopathological characteristics and dUTPase expression status. Univariate and multivariate Cox proportional hazards regression analysis was used to evaluate the association of dUTPase expression and clinicopathological parameters with patient outcome. All statistical analyses were performed using SPSS software (SPSS software package; SPSS Inc., Chicago, IL, USA) and GRAPHPAD PRISM software (GraphPad Software Inc., La Jolla, CA, USA).

Results

Gene expression profiling identified the overexpression of *DUT* in hepatocellular carcinoma

To overcome the considerable individual variability of transcriptomic characteristics, we constructed a SAGE library of normal human liver using RNAs derived from five normal liver tissues. In addition, we constructed two SAGE libraries derived from three HCC tissues or corresponding non-cancerous liver tissues from patients who developed HCC with a history of chronic hepatitis C. We detected a total of 226 267 tags corresponding to 45 746 unique tags from these SAGE libraries (supporting information Table S1). After excluding the tags detected only once in each library, we selected 15 333 reliable unique transcripts expressed in at least one of the SAGE libraries to avoid contamination of tags derived from sequence errors. Then, we annotated these transcripts using SAGE Genie database and the Source database to identify the potential subcellular localization of transcripts categorized into eight groups in each SAGE library.

The number of nuclear component-related transcripts was increased in the HCC library compared with the normal liver and non-cancerous liver libraries, whereas the other cellular component-related transcripts did not show this tendency (supporting information Fig. S1). Because nuclear component-related genes may closely correlate with cancer cell proliferation and chemosensitivity (24), we further investigated the expression of nuclear component-related tags in

each library, and identified 10 transcripts associated with nucleotide/nucleoside metabolism that are over-expressed in HCC (Table 1). Using Monte Carlo simulation, we evaluated the significance of differentially expressed transcripts in HCC and corresponding CLD libraries or in HCC and normal liver libraries. We identified a *DUT* gene encoding dUTPase (dUTPase) whose expression was significantly altered ($P=0.01$). We also identified a *TS* gene encoding thymidylate synthase in the list, but the difference did not reach statistical significance.

dUTPase is a phosphatase known to maintain a dUMP pool by catalysing the hydrolysis of dUTP to dUMP, and thus provides a substrate of thymidylate synthase. Its role in HCC is unknown; therefore, we examined *DUT* expression in 20 independent HCC and corresponding non-cancerous liver tissues, and identified significant overexpression of *DUT* in HCC tissue ($P=0.0015$) (Fig. 1A). Moreover, we detected more than a two-fold increase in *DUT* expression in 70% of HBV-related and HCV-related HCC cases (14 of 20 HCCs) compared with the non-cancerous liver tissues (Fig. 1B). We further examined the expression of *DUT* in 238 HCC tissues compared with the non-cancerous liver tissues using publicly available microarray data (GSE5975) (Fig. S2). Consistent with the SAGE data, *DUT* was overexpressed more than two-fold in 121 of 238 HCC tissues (median: 2.03), whereas *TS* was overexpressed more than two-fold in 54 of 238 HCC tissues (median: 1.41) compared with the non-cancerous liver tissues.

Pivotal role of dUTP pyrophosphatase expression in cell proliferation in hepatocellular carcinoma cell lines

In general, cancer gene signatures discovered by comparison between tumour and non-tumour tissues are more likely to reflect the differences in the control of cell proliferation and growth (25). Accordingly, we investigated the function of dUTPase in cell proliferation in HuH7 cells by *DUT* gene knockdown. *DUT* expression was decreased by 60–70% following the transfection of the siRNA constructs specifically targeting *DUT* 48 h after transfection (*DUT*1 in Fig. 2A and *DUT*2 in Fig. S3A), and cell growth was significantly inhibited compared with the control 72 h after transfection (Fig. 2B and Fig. S3B). Anchorage-independent cell growth was also significantly impaired by *DUT* gene knockdown 14 days after transfection (Fig. 2C). Furthermore, *DUT* gene knockdown decreased the numbers of both migrating and invading cells 72 h after transfection (Fig. 2D and E).

dUTPase is known to be associated with thymidylate synthesis (26), and thus we evaluated the effects of 5-FU, a thymidylate synthase inhibitor, on dUTPase expression in HCC cell lines *in vitro*. When we treated HuH7 cells with low-dose 5-FU (0.25 mg/ml), we could not detect any growth-inhibitory effects (Fig. 2F). Based on this condition, we evaluated the effect of *DUT* gene knockdown on 5-FU sensitivity 72 h after transfection.

Table 1. Genes associated with nucleic acid metabolism overexpressed in hepatocellular carcinoma

Tag sequence	Normal liver	Non-cancerous liver	HCC	Fold*	Gene	P-value†
CAGCTCCGCT	0	2	11	5.5	dUTP pyrophosphatase	0.010
AAAGGATAAT	0	0	3	> 3	General transcription factor II H, polypeptide 2	0.127
ACGGTCCAGG	0	0	3	> 3	Cytidine deaminase	0.127
ATGTAGAGTG	0	0	3	> 3	Thymidylate synthase	0.127
TGGGGATTAC	1	0	3	> 3	Zinc ribbon domain containing, 1	0.127
CACCCTGTAC	2	2	6	3	Solute carrier family 29	0.147
GAACGCCTAA	1	1	3	3	Dihydropyrimidinase-like 2	0.308
GCGCTGGTAC	0	1	3	3	2'-5'-oligoadenylate synthetase 3	0.308
CTTAGTGCAA	0	2	4	2	3'-phosphoadenosine 5'-phosphosulphate synthase 2	0.335
TTGTACATC	0	2	3	1.5	Phosphoribosyl pyrophosphatase synthetase-associated protein 1	0.506

*Fold increase was calculated by dividing the number of tags in HCC by that of tags in non-cancerous liver. To avoid division by 0, a tag value of 1 was used for any tag that was not detectable in one sample.

†Statistical significance of differentially expressed genes between two groups (HCC and non-cancerous liver libraries) was calculated using Monte Carlo simulation.

HCC, hepatocellular carcinoma.

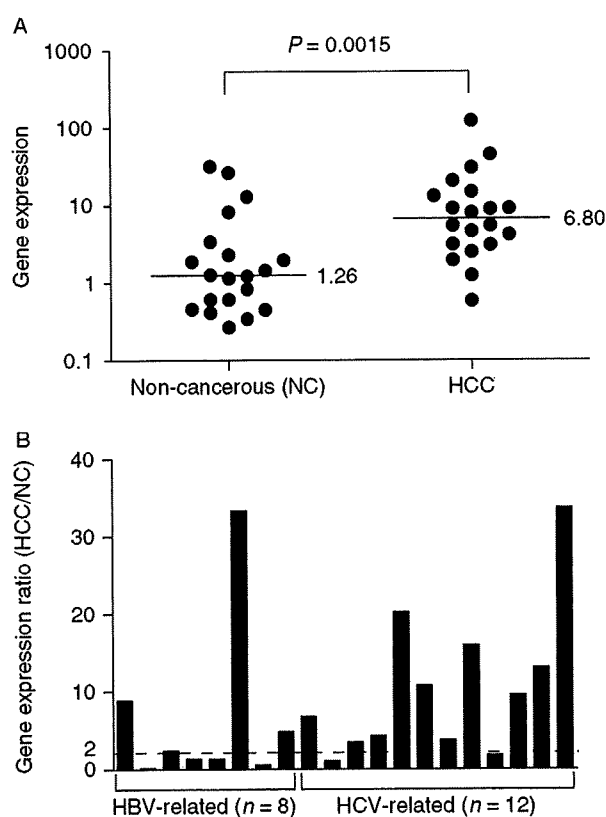


Fig. 1. (A) Quantitative reverse transcription-polymerase chain reaction analysis of *DUT* expression in hepatocellular carcinoma (HCC) and corresponding non-cancerous liver tissues. *DUT* was significantly activated in HCC tissues compared with non-cancerous liver tissues ($P = 0.0015$). A median value in each group is indicated. (B) *DUT* gene expression ratios of HCC and corresponding non-cancerous liver tissues. Fourteen of 20 HCC tissues expressed *DUT* more than two-fold compared with the background non-cancerous liver tissues. HBV, hepatitis B virus; HCV, hepatitis C virus.

Interestingly, *DUT* gene knockdown not only suppressed cell proliferation but also sensitized HuH7 cells to low-dose 5-FU (Fig. 2F and Fig. S3B). These data suggest that dUTPase overexpression in HCC tissues may be associated with enhanced cell proliferation and 5-FU resistance.

Intense dUTP pyrophosphatase expression is correlated with a poor prognosis in hepatocellular carcinoma patients

To characterize the clinicopathological characteristics of dUTPase expression in HCC, we performed IHC using an additional independent HCC cohort. Accordingly, we explored the dUTPase expression in HCC using 82 formalin-fixed paraffin-embedded HCC specimens. All HCC tissues were surgically resected at the Liver Disease Center of Kanazawa University Hospital with full clinical information, and their immunoreactivity to anti-dUTPase antibodies was evaluated by IHC. We noticed that anti-dUTPase antibodies reacted to both nuclear (red arrows) and cytoplasmic (blue arrows) isoforms of dUTPase, as described previously (26) (Fig. 3A and B). We therefore evaluated the nuclear and cytoplasmic expression of dUTPase separately. We stratified HCC tissues and evaluated the dUTPase expression status based on the percentages of dUTPase-positive cells. The frequency of nuclear or cytoplasmic dUTPase-positive cells was highly variable in each HCC tissue, and we defined HCCs with nuclear or cytoplasmic dUTPase expressed in $\geq 50\%$ of tumour cells as nuclear or cytoplasmic dUTPase-high HCC (Fig. 3C). Nuclear dUTPase overexpression was detected in 36.6% (30 of 82), whereas cytoplasmic dUTPase overexpression was detected in 67.1% (55 of 82) of HCC tissues compared with the corresponding non-cancerous liver tissues

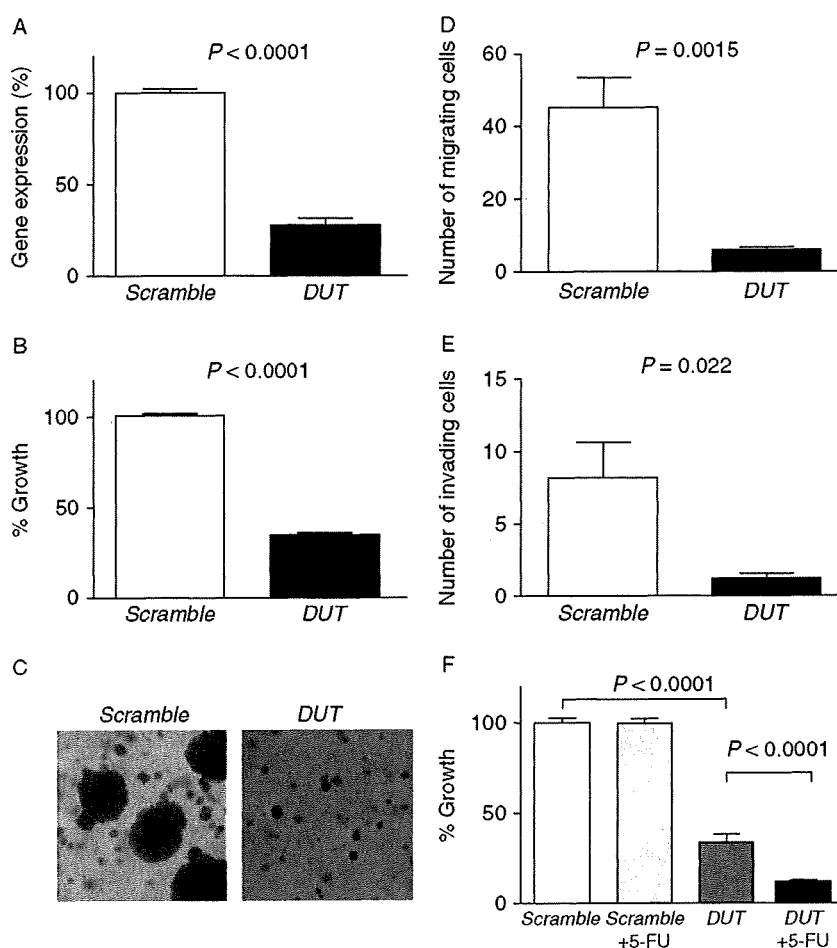


Fig. 2. (A) Transfection of small interfering RNAs targeting *DUT* (*DUT1*) decreased *DUT* expression compared with the control (scrambled sequence). Gene expression was evaluated in triplicate 72 h after transfection (mean \pm SD). (B) *DUT* gene knockdown significantly suppressed cell proliferation ($P < 0.0001$). Cell viability was evaluated in triplicate 72 h after transfection (mean \pm SD). (C) Soft agar assay. *DUT* gene knockdown suppressed anchorage-independent cell growth. (D and E) Matrigel invasion assay. *DUT* gene knockdown decreased the numbers of both migrating and invading cells. Experiments were performed in triplicate (mean \pm SD). (F) *DUT* gene knockdown sensitized HuH7 cells to low-dose 5-fluorouracil (5-FU) (0.25 μ g/ml), which had no effect on the cell proliferation in the control (mean \pm SD).

(Table 2). In general, non-cancerous hepatocytes rarely expressed nuclear dUTPase (Fig. 3A).

We investigated the clinicopathological characteristics of nuclear or cytoplasmic dUTPase in low/high HCC cases (Table 2). The expression status of nuclear dUTPase showed no correlation with age, gender, virus, presence of cirrhosis, α -fetoprotein value, tumour size and TNM stages. However, nuclear dUTPase expression was significantly correlated with the histological grades of HCC ($P = 0.0099$), and high frequencies of nuclear dUTPase-positive cells were associated with poorly differentiated cell morphology in the HCC tissue. In contrast, cytoplasmic dUTPase expression was not correlated with the histological grades of HCC ($P = 0.077$). We examined the cell proliferation of these HCC samples by PCNA staining, and PCNA indexes were significantly higher in nuclear dUTPase high HCC than low HCC with statistical significance ($P = 0.01$) (Fig. S4).

We further investigated the prognostic significance of dUTPase expression in HCC. Strikingly, high nuclear dUTPase expression in HCC tissue correlated with a poor survival outcome compared with low nuclear dUTPase expression ($P = 0.0036$), whereas high cytoplasmic dUTPase expression had little effects when evaluated by recurrence-free survival (Fig. 3D). Furthermore, univariate Cox regression analysis showed a significant correlation between high nuclear dUTPase expression and a high risk of mortality (HR, 2.47; 95% CI, 1.08–5.66; $P = 0.032$; Table 3). By multivariate Cox regression analysis, TNM stage (HR, 2.75; 95% CI, 1.11–6.79; $P = 0.027$) and nuclear dUTPase (HR, 2.61; 95% CI, 1.13–6.05; $P = 0.024$) were independent prognostic factors associated with a high risk of mortality, and other clinicopathological features did not add independent prognostic information. These data indicate a significant correlation between the malignant potential of